ISTANBUL TECHNICAL UNIVERSITY ★ GRADUATE SCHOOL

NUMERICAL INVESTIGATION OF THERMAL COMFORT FOR PASSENGERS IN A HELICOPTER CABIN

M.Sc. THESIS

Mehmet KÜLTE

Department of Mechanical Engineering

Heat and Fluid Programme

JUNE 2025

ISTANBUL TECHNICAL UNIVERSITY ★ GRADUATE SCHOOL

NUMERICAL INVESTIGATION OF THERMAL COMFORT FOR PASSENGERS IN A HELICOPTER CABIN

M.Sc. THESIS

Mehmet KÜLTE
(503221110)

Department of Mechanical Engineering

Heat and Fluid Programme

Thesis Advisor: Assoc. Prof. Sertaç ÇADIRCI

JUNE 2025

İSTANBUL TEKNİK ÜNİVERSİTESİ ★ LİSANSÜSTÜ EĞİTİM ENSTİTÜSÜ

HELİKOPTER KABİNİ İÇERİSİNDEKİ YOLCULAR İÇİN TERMAL KONFORUN SAYISAL ARAŞTIRMASI

YÜKSEK LİSANS TEZİ

Mehmet KÜLTE
(503221110)

Makina Mühendisliği Anabilim Dalı

Isı Akışkan Programı

Tez Danışmanı: Doç. Dr. Sertaç ÇADIRCI

HAZİRAN 2025

Mehmet Külte, a M.Sc. student of ITU Graduate School student ID 503221110, succesfully defended the thesis/dissertation entilted "NUMERICAL INVESTIGATION OF THERMAL COMFORT FOR PASSENGERS IN A HELICOPTER CABIN" which he prepared after fulfilling the requirements specified in the associated legislations, before the jury whose signatures are below.

Thesis Advisor : **Assoc. Prof. Dr. Sertaç ÇADIRCI** ....
Istanbul Technical University

Jury Members : **Prof. Dr. Yakup Erhan BÖKE** ....
Istanbul Technical University

Prof. Dr. Derya Burcu ÖZKAN ....
Yıldız Technical University

Date of Submission : 26.05.2025
Date of Defense : 20.06.2025

To my family,

FOREWORD

I hope that the outcome of this thesis study will contribute positively to the industry, especially in our country, and that I will be able to serve my country as a valuable engineer with the knowledge and experience I have gained throughout my education.

I would like to sincerely thank my family, who have always supported me throughout my life.

I would like to express my gratitude to my colleagues at TUSAŞ who supported me in helicopter thermal studies both during and prior to my thesis process. I would also like to extend my special thanks to my thesis advisor, Assoc. Prof. Sertaç ÇADIRCI, for his continuous support throughout the thesis period.

I would also like to express my gratitude to TUSAŞ and its employees for providing me with the opportunity and resources to conduct the CFD analyses throughout this thesis.

May 2025

Mehmet KÜLTE
(Mechanical Engineer)

TABLE OF CONTENTS

Page

ABBREVIATIONS

ARP : Aerospace Recommended Practice
CFD : Computational Fluid Dynamics
CFRP : Carbon Fiber Reinforced Polymer
CS : Certification Specification
ECS : Environmental Control Systems
EDT : Effective Draft Temperature
ET : Equivalent Temperature
PIV : Particle Image Velocimetry
PMV : Predicted Mean Vote
PPD : Predicted Percentage of Dissatisfied
RNG : Renormalization Group
SAE : Society of Automotive Engineers
SST : Shear Stress Theory

SYMBOLS

C	**:** Celcius
I	**:** Isolation
K	**:** Kelvin
k	**:** Turbulance Kinetic Energy
m	**:** Meter
P	**:** Pressure
v	**:** Velocity
W	**:** Watt
ω	**:** Spesific Dissipation Rate
ρ	**:** Density

LIST OF TABLES

Page

LIST OF FIGURES

Page

NUMERICAL INVESTIGATION OF THERMAL COMFORT FOR PASSENGERS IN A HELICOPTER CABIN

SUMMARY

In this thesis, the comfort of passengers inside a helicopter cabin and the parameters affecting this comfort are numerically investigated. Ensuring the comfort of both pilots and passengers in aerial vehicles is crucial for the safe continuation of operations. Air distribution systems play a vital role in providing a safe, healthy, and comfortable cabin environment in aircraft. Achieving a uniform air velocity and temperature distribution in complex structures like helicopter cabins is a challenging task. For maintaining a homogeneous environment within the cabin, it is essential to carefully determine the positions and flow rates of air outlets. Low airspeeds and high temperatures inside the cabin can lead to discomfort among passengers.

Helicopters can be designed differently depending on their intended use and the missions they are assigned. While the cockpit typically accommodates two pilots, the cabin section may vary in passenger capacity according to the design. Despite design variations, certain standards must be met for each aerial vehicle, and these are defined in the literature. SAE ARP292, ASHRAE 161-2013, and ASHRAE 161-2007 are some of the key standards that aircraft are expected to comply with. This thesis presents the significant outputs of these standards.

The study begins with a comprehensive literature review. Existing research on aircraft, especially airplanes, mainly focuses on thermal comfort. Both experimental and numerical studies typically address the positioning of air outlets and their effects. One of the previous experimental studies found in the literature is reproduced using the commercial computational fluid dynamics software, Star-CCM+, and the results are validated. Velocity distributions in specific regions of the flow domain are analyzed to form the necessary foundation for this study. Due to the lack of infrastructure for experimental research and the high costs associated with testing multiple parameters, the study continued solely as a numerical investigation.

The analyses are conducted in a three-dimensional, steady-state environment. The helicopter cabin examined in this thesis has dimensions of 3900-2600-1700 mm. Inside the cabin, there are four passengers and their seats. The helicopter cabin has a complex geometry, and simplifications are made to maintain its fidelity. Avionic equipment and their thermal loads are neglected. The analyses are performed under extreme ambient temperature and solar radiation conditions. The ambient temperature is assumed to be 50 °C, with the helicopter considered stationary, representing the most challenging environmental scenario. Cold air is supplied through individual air outlets (known as gaspers) and main outlets to maintain a moderate cabin temperature and ensure passenger thermal comfort. The cabin includes four individual air outlets and two fixed main outlets.

According to CS 29.841 ventilation requirements, all passenger and crew compartments must be adequately ventilated. Specifically, each crew compartment must be supplied with sufficient clean air to allow crew members to perform their duties without excessive discomfort or fatigue, at least 0.3 m³ per minute per crew member. Air supplied through gaspers and main outlets meets the requirement for clean air and helps regulate cabin temperature. Even if all gaspers are completely closed, the airflow provided through the fixed outlets is sufficient to meet the standard.

This thesis investigates the thermal comfort of passengers by examining the effect of different parameters. The thermal comfort of passengers is evaluated using Equivalent Temperature (ET) and Effective Draft Temperature (EDT) for various parameter sets. By comparing ET and EDT values across different body regions, the relative importance of convective and radiative heat transfer in determining cabin comfort is emphasized. Passenger body parts, including the head, left arm, right arm, shoulders, torso, left leg, and right leg, were examined based on average ET and EDT values to assess comfort levels.

The first parameter examined is the positioning of the gaspers. Gasper units are placed above passengers, and the angle at which air is delivered to passengers is assumed to be fixed. Alternative gasper positions are defined 90 mm away from the reference gasper location to allow comparison. Analyses revealed that the most suitable gasper position iss directly aligned with the vertical centerline of the passenger's body, at a distance of 0–30 mm from the head region. This optimal design is adopted for the rest of the analysis sets to ensure consistent thermal comfort for passengers.

The second parameter involved varying the airflow ratio between gaspers and fixed outlets to assess the contribution of gasper airflow to thermal comfort. In this analysis set, the total airflow rate was kept constant, while the percentage of airflow through gaspers is changed to 100%, 75%, 50%, 25%, and 0%. The results showed that decreasing the airflow through gaspers led to reduced passenger thermal comfort, thus highlighting the positive impact of gaspers on comfort.

The third parameter focused on the effect of gasper cross-sectional area on thermal comfort. If the airflow rate from gaspers remains constant, according to the principle of mass conservation, reducing the outlet area increases airflow velocity. Since gaspers function as jet nozzles, a reduced cross-section results in higher localized velocities near passengers. The analyses demonstrated that while reduced outlet area positively contributes to thermal comfort, excessive localized airflow velocity could be detrimental. Therefore, the outlet area must be carefully selected to maintain comfortable airspeeds.

The fourth parameter examined the relationship between the ambient air temperature and the temperature of air supplied through gaspers and fixed outlets. In previous analyses, 10 °C cold air is supplied while the ambient temperature is kept constant at 50 °C. In this parameter set, ambient temperatures are varied to 50 °C, 48 °C, 46 °C, 44 °C, 42 °C, and 40 °C, and the appropriate supply air temperatures are adjusted accordingly to ensure passenger comfort. The results confirmed that air temperature can be adjusted in correlation with ambient conditions.

In conclusion, this thesis investigated various parameters affecting passenger thermal comfort in a helicopter cabin. Evaluations are conducted based on the average ET and EDT values of different body regions, and the impacts of different design and environmental variables are thoroughly analyzed.

HELİKOPTER KABİNİ İÇERİSİNDEKİ YOLCULARIN TERMAL KONFORUNUN SAYISAL OLARAK İNCELENMESİ

ÖZET

Bu tezde, helikopter kabini içerisindeki yolcuların konforu ve yolcuların konforunu etkileyen parametreler numerik olarak incelenmiştir.

Hava araçlarında pilot ve yolcuların konforunun sağlanması operasyonun sağlıklı şekilde devam ettirilebilmesi adına önem taşımaktadır. Hava dağıtım sistemleri hava araçlarında güvenli, sağlıklı ve rahat kabin ortamı yaratılması adına kritik öneme sahiptir. Helikopter kabini gibi karmaşık yapılarda homojen hava hızı ve sıcaklığı elde edilmesi oldukça zorlu bir görevdir. Kabin içerisinde homojen ortamın sağlanması için için hava çıkışlarının konumlarının ve debilerinin dikkatlice belirlenmesi büyük önem taşımaktadır. Kabin içerisindeki düşük hava hızları ve yüksek sıcaklıklar, yolcular arasında rahatsızlık hissine neden olabilmektedir.

Helikopterler kullanım amaçlarına ve üstlendiği görevlere göre farklı tasarımlara sahip olabilir. Kokpit bölgesinde iki pilot ve kabin bölgesinde tasarımlarına göre farklı yolcu kapasitesine sahip olabilir. Her ne kadar tasarımlar birbirinden farklı olsa da her bir hava aracının uygun olması gereken standartlar literatürde mevcuttur. SAE ARP292, ASHRAE 161-2013 ve ASHRAE 161-2007 hava araçlarının sağlaması gereken bazı standartlardır. Tez içerisinde bu standartların önemli çıktıları aktarılmıştır.

Tez çalışmasına öncelikli olarak literatur taraması yapılarak başlanmıştır. Literatürde hava araçları özellikle uçaklar özelinde termal konfor çalışmaları yer almaktadır. Deneysel ve numerik çalışmalar genellikle hava çıkış konumlarının belirlenmesi ve etkilerinin incelenmesi üzerine olmaktadır. Ardından literatürde yer alan ve önceden gerçekleştirilen deneysel çalışmalardan birisi ticari hesaplamalı akışkanlar dinamiği çözücüsü olan Star CCM+ yazılımı ile tekrar çözülmüş, doğrulaması yapılmış ve akış hacminin belirli bölgelerindeki hız dağılımları incelenerek çalışma için gerekli altyapı oluşturulmuştur. Deneysel çalışmalar için gerekli altyapının olmayışı, incelenecek her bir parametre için maliyetlerin yüksek olması sebebiyle çalışma numerik olarak devam etmiş ve deneysel olarak inceleme yapılmamıştır.

Analizler üç boyutlu, zamandan bağımsız ortamda yapılmıştır. Tezde incelenen helikopter kabini 3900-2600-1700 mm boyutlarındadır. Kabin içerisinde 4 yolcu ve yolcuların koltukları bulunmaktadır. Helikopter kabini karmaşık bir geometriye sahiptir ve aslına uygun olacak şekilde sadeleştirmeler yapılmıştır. Kabin içerisindeki aviyonik ekipmanlar ve ekipmanların ısıl yükleri ihmal edilmiştir. Helikopter için en zorlu sıcaklık ve güneş yükü koşulları altında analizler gerçekleştirilmiştir. Helikopterin bulunduğu ortam sıcaklığı 50 °C ve durgun ortamda olduğu kabulü yapılmış ve en zorlayıcı ortam için analizler gerçekleştirilmiştir. Helikopter kabini içerisinde gasper adı verilen bireysel hava çıkışları ve ana çıkışlardan soğuk hava sağlanarak kabin ortalama sıcaklığı belli seviyelerde tutulmaya çalışılmış ve yolcuların

termal konforunun sağlanması amaçlanmıştır. Kabinde dört bireysel hava çıkışı ve iki sabit hava çıkışı bulunmaktadır.

CS 29.841 havalandırma gerekliliklerine göre, tüm yolcu ve mürettebat bölmeleri yeterli şekilde havalandırılmalıdır. Özellikle, her mürettebat bölmesine mürettebat üyelerinin aşırı rahatsızlık veya yorgunluk yaşamadan görevlerini yerine getirebilmelerini sağlamak için yeterli miktarda temiz hava sağlanmalıdır - mürettebat üyesi başına dakikada en az 0,3 m³'tür. Gaspers ve ana çıkışlardan gelen hava, temiz hava gereksinimlerini karşılamaya ve kabin sıcaklığını düzenlemeye yardımcı olur. Sabit hava çıkışlarından kabine sağlanan hava debisi CS 29.841 gereksinimini karşılamaktadır. Gasper'ların tamamen kapatılması durumunda dahi gereksinim sağlanmaktadır.

Tezde kabin içerisindeki yolcuların termal konforları farklı parametrelerin değişimi ile incelenmiştir. Yolcuların termal konforu, farklı parametreler için Eşdeğer Sıcaklık (ET) ve Etkili Sürükleme Sıcaklığı (EDT) kullanılarak değerlendirilmiştir. Yolcuların vücutlarının farklı bölgelerindeki ET ve EDT değerleri karşılaştırılarak, helikopter kabini içerisindeki termal konforun belirlenmesinde sürüklenme ve radyasyonla ısı transferinin göreceli önemi vurgulanmıştır. Yolcuların kafa, sol kol, sağ kol, omuz, gövde, sol bacak ve sağ bacak bölgeleri ET ve EDT sıcaklık ortalamaları incelenerek yolcuların termal konforu irdelenmiştir.

İncelenen ilk parametre gasper konumunun belirlenmesidir. Gasper'lar yolcuların üst kısımlarına konumlandırılmıştır ve yolculara hava geliş açısı sabit kabul edilmiştir. Referans olarak kabul edilen gasper konumunun 30 mm uzaklığında kıyas amaçlı yeni gasper konumları belirlenmiş ve analizler gerçekleştirilmiştir. Analizler sonucunda en uygun gasper konumu yolcu vücudunun sağ ve sol yarısının simetriğinde, kafa bölgesinden 0-30 mm uzaklıkta olduğu belirlenmiştir. Böylece diğer analiz setleri için yolcuların termal konforunu sağlayacak en uygun tasarım tespit edilmiştir.

İncelenen ikinci parametre gasper ve sabit hava çıkış oranları değiştirilerek gasper hava çıkışının termal konfora etkisi incelenmiştir. Bu parametre setinde gasper ve sabit hava çıkışlarındaki toplam hava debisi aynı olacak şekilde analizler gerçekleştirilmiştir. Gasper'lardan kabine sağlanan hava debisi oranı %100, %75, %50, %25 ve %0 olacak şekilde analizler gerçekleştirilmiş ve yolcuların termal konforu incelenmiştir. Analizler sonucunda gasper'lardan sağlanan hava debisi oranı azaldıkça yolcuların termal konforunda azalma görülmüştür ve böylece gasper'ların termal konfora olan olumlu etkisi ortaya konmuştur.

İncelenen üçüncü parametre gasper kesit alanı değişiminin termal konfora etkisinin incelenmesidir. Gasper'lardan sağlanan hava debisi aynı kalması durumunda, kütlenin korunumu prensibine göre, hava çıkış kesit alanının azalması ile hava hızının arttığı bilinmektedir. Gasper'lar prensip gereği jet akışı sağlamaktadır. Dolayısıyla kesit alanının azalması ile yolcu üzerinde lokal olarak yüksek hava hızı değerleri görülmektedir. Analizler sonucunda kesit alanının azalması termal konfora pozitif etkisi bulunmaktadır ancak yolcu üzerinde yüksek hava hız akışı sağlanması konforu negatif etkileyeceğinden kesit alanını hava hızının rahatsız etmeyecek seviylerde tutulması gerekmektedir.

İncelenen dördüncü parametre dış ortam hava sıcaklığına göre gasper ve sabit hava çıkışlarından kabin içine sağlanan hava sıcaklığının incelenmesidir. Analizler diğer üç incelemede 50 °C ortam hava sıcaklığına göre 10 °C soğuk hava sıcaklığının sağlanarak incelenmişti. Bu parametrede ortam sıcaklıkları 50 °C, 48 °C,46 °C, 44 °C, 42 °C ve 40 °C olacak şekilde iç ortama sağlanan hava sıcaklığının yolcuların termal konforu sağlanacak şekilde yeniden belirlenmesidir. Sonuç olarak dış ortam sıcaklığına göre soğuk hava sıcaklığının belirli bir korelasyona göre ayarlanabildiği gösterilmiştir.

Bu tezde, helikopter kabini içerisinde yolcuların termal konforunu etkileyen parametreler incelenmiştir. Termal konfor, yolcuların vücut bölgelerindeki ortalama ET ve EDT sıcaklık değerleri üzerinden çıkarımlar yapılmış ve parametrelerin etkileri incelenmiştir.

1. INTRODUCTION

Comfort plays a vital role in safeguarding individuals' physical and mental health, improving productivity, and sustaining overall quality of life. The environmental conditions of living and working spaces have a direct impact on human performance. Environments that prioritize thermal, acoustic, and ergonomic comfort contribute to improved concentration, reduced stress, and greater overall productivity. Therefore, improving comfort standards across sectors including education, healthcare, transportation, and industry, can elevate service quality and user satisfaction. Conversely, discomfort in any setting may lead to exhaustion, decreased concentration, and a sense of dissatisfaction, negatively affecting both personal well-being and organizational success. Therefore, incorporating comfort-related criteria into the design of buildings and vehicles is not merely a matter of convenience but a fundamental requirement that supports both user-centered design and sustainable development goals.

Comfort is a multifaceted concept that significantly influences individuals' physical health, emotional well-being, and cognitive functioning. According to Frontczak et al. (2011), comfort in indoor environments is not limited to thermal conditions but also includes acoustic, visual, and air quality factors, all of which collectively shape human perception, satisfaction, and performance. These environmental aspects directly impact how effectively individuals can concentrate, communicate, and carry out tasks in both personal and professional settings. The provision of comfort, especially in terms of thermal comfort and air quality, is critical in both residential and vehicular environments. In homes, comfort is achieved through systems for heating, cooling, ventilation, and insulation. In closed environments such as offices and public buildings, factors like air quality, humidity control, and ventilation are vital in maintaining a comfortable atmosphere, which has a direct impact on occupants' well-being and productivity. Similarly, in vehicles, comfort is ensured through systems like air conditioning, seat heating and cooling, and vibration-reducing suspensions. Proper air circulation and temperature regulation are essential for providing a pleasant journey, particularly on long trips. Advanced air filtration systems also play a significant role in maintaining clean and fresh air inside the vehicle.

In air vehicles, maintaining optimum comfort within the limited cabin space becomes even more essential. This requires precise control of temperature, humidity, and airflow to guarantee that passengers have a pleasant and comfortable experience during their flight. Wang et al. (2024) highlight the importance of maintaining a balance between thermal comfort and indoor air quality, emphasizing that even small fluctuations in these parameters can affect passenger well-being during flight. Personal air supply systems, such as individualized air outlets which are gaspers, are crucial in meeting the diverse thermal comfort and air quality needs of each passenger. These personalized systems allow for tailored comfort without affecting others, improving the overall passenger experience.

of new However, existing standards currently lack specific guidelines regarding the appropriate airflow rates for nozzles in aircraft cabins. Given the significant impact of passenger comfort on the civil aviation industry where higher satisfaction directly translates into improved profitability this gap warrants further investigation and development. The growing emphasis on cabin environment and comfort in recent years highlights the need for effective solutions, with thermal comfort remaining a key design criterion in the development aircraft. Helicopter thermal comfort is one of the aspects that shall be examined within aircraft.

A helicopter, when examined as a whole, exhibits a highly complex structure. Each component, such as the cockpit, cabin, pylon section, rotors, blades, tail section, and landing gear, presents its own set of complexities and structural challenges. In most helicopters, the cockpit and cabin are not distinctly separated, although some models feature a structural division between these sections. The cockpit houses the pilots, their seats, the control panel, electronic systems, and other critical operational elements. The cabin, on the other hand, accommodates the passengers, their seating arrangements, functional equipment tailored to the helicopter’s specific use, and additional structural components. The layout of the cabin can vary significantly based on the helicopter's intended function. For example, medical helicopters are often equipped with stretchers for patients, medical units, and other specialized equipment to assist healthcare personnel. In contrast, military helicopters are designed with seating and interior configurations that cater to the specific demands of military operations.

Thermal comfort in aircraft cabins depends on various parameters, which can be categorized as personal and environmental factors. Personal factors include the metabolic rate of occupants and the thermal insulation provided by clothing, both of which affect how individuals perceive temperature changes within the cabin. Environmental factors, primarily controlled by the aircraft's Environmental Control System (ECS), include air temperature, velocity, humidity, and radiation effects from the cabin's walls, windows, and onboard equipment. The design and placement of air supply inlets, airflow distribution, and heat loads generated by passengers and onboard systems are also critical factors influencing the thermal comfort within the cabin. Thermal comfort in aircraft cabins is closely linked to environmental variables such as air temperature, humidity, and airflow patterns.

According to According to the European Union Aviation Safety Agency (EASA, 2024), CS 29.861 ventilation requirements, all passenger and crew compartments must be adequately ventilated. In particular, each crew compartment must be provided with a sufficient supply of fresh air—not less than 0.3 m^3 (10 cubic feet) per minute per crew member—to ensure that crew members can carry out their duties without experiencing excessive discomfort or fatigue. The air from the gaspers and main outlets helps to meet the fresh air requirements and regulate the cabin temperature.

One of the most significant parameters determining thermal comfort within an aircraft is air distribution. In complex structures like helicopters, where temperature distribution may not be uniform, it is essential that the air distribution system be designed to ensure comfort. Key factors influencing passenger comfort in the helicopter cabin include the speed of the air directed over the passenger, the ambient temperature, and the temperature in the immediate area surrounding the passenger. Standards outlined in the literature, such as SAE ARP292 (2003) and ASHRAE (2007), provide guidelines for air velocity and comfort in aircraft cabins. SAE ARP292 (2003), which governs airflow rates in passenger cabins, recommends that air speeds at seat level should be at least 1 m/s. Air outlet speeds between 1 m/s and 3 m/s are generally regarded as optimal for maintaining both thermal comfort and air quality.

Additionally, ASHRAE (2007) recommends a minimum air velocity of 1 m/s at the head level of air outlets to ensure the effectiveness of personal air outlets.

In recent years, advancements in technology have expanded the applications and capabilities of CFD. As calculation times have shortened and available resources have increased, the accuracy of CFD simulations has improved. Within this study, the thermal comfort of passengers in the helicopter cabin was analyzed using the Star CCM+ CFD software. By identifying key parameters influencing thermal comfort, optimal locations for individual air outlets are determined, providing valuable insights into improving passenger comfort in aircraft. In the thesis, the parameters affecting comfort are examined with CFD analysis numerically.

2. LITERATURE REVIEW

In this section, a literature review of studies on thermal comfort in aircraft is presented. The literature includes not only studies on thermal comfort in helicopter cabins, which is also the focus of this work, but also experimental and numerical studies conducted on other types of aircraft. Experimental studies on aircraft have focused on mock-up designs. This section reviews studies related to the necessary criteria for ensuring passenger comfort in aircraft and the characteristics of these criteria.

Kühn et al. (2009) conducted a study where forced and mixed convection are experimentally investigated in a full-scale mock-up of an A380 passenger aircraft cabin. The study demonstrates that the flow field in aircraft cabins is influenced by various fluid mechanical phenomena. The interaction between the supplied air jets, the negative buoyancy forces acting on these jets, and the interaction of thermal plumes with the supplied air jets all play a significant role in shaping the flow field within the cabin.

Bosbach et al. (2006) studied the airflow within an A380 cabin mock-up under isothermal conditions. They compared simulation results with experimental data gathered using the PIV technique and concluded that low Reynolds number models provide accurate predictions of jet diffusion and separation. As a result, their study recommended that using low Reynolds number models instead of high Reynolds number and two-layer models for isothermal cabin flow simulations.

Lui et al. (2012) stated that UAs are a reliable method for measuring three-dimensional air velocity, turbulence kinetic energy, and turbulence intensity. Their study found that the air supply from the side diffusers created large recirculation zones on both sides of the cabin. However, the overall airflow was not completely symmetrical due to asymmetrical air distribution and unexpected airflow in the upper region.

According to Yan et al. (2009), airborne pollutants in an aircraft cabin are greatly affected by the airflow produced by the ventilation system, which divides the airflow into two separate halves. As a result, the majority of pollutants stay within the half where they are released, with little cross-contamination across the central axis. Furthermore, the position of the pollutant source plays a vital role in its distribution. Pollutants emitted near the air outlets have a lesser impact on cabin air quality compared to those released in the middle region.

Li et al. (2015) conducted experimental and Computational Fluid Dynamics (CFD) analyses on a cabin mock-up. In their study, they observed that velocity data measured separately in vertical and horizontal directions aligned well with the analysis results. Measuring velocity components individually along these axes yielded accurate outcomes.

Wang et al. (2017) conducted an analysis of the instantaneous airflow within an aircraft cabin mock-up, focusing on the collision regions formed by interacting jets. They studied turbulence scales, spectral characteristics, and energy distribution to gain a deeper understanding of the airflow dynamics in these areas. The study's findings revealed that the collision regions of jets within an aircraft cabin feature turbulent airflow with low velocity magnitudes and high fluctuations. Although the mean airflow fields are uniform with small velocity gradients, the instantaneous airflow fields exhibit significant instability.

Zhang et al. (2007) conducted a comparative study on commercial aircraft, assessing individual ventilation systems in comparison to traditional ventilation methods. The personalized air distribution system resulted in the lowest CO_2 concentrations in the breathing zone, with slightly lower air temperatures than the other two systems, while avoiding significant draft risks. By supplying outside air directly to the breathing zone, this system effectively reduced the risk of airborne infectious disease transmission within the cabin.

You et al. (2016) compared the results of tests and CFD analyses to examine airflow in a mock-up cabin geometry. The study concluded that the k-ω SST turbulence model provided more accurate results compared to the k-ε RNG model.

In the study conducted by Zvar Bašković et al. (2014), the airflow within the passenger compartment of an electric vehicle was numerically investigated, and the performance of different turbulence models and near-wall treatment approaches was evaluated. Simulations were performed using the standard k–ε, RNG k–ε, and SST k–ω turbulence models. Among these, the SST k–ω model demonstrated superior accuracy in capturing the near-wall boundary layer behavior. Furthermore, when combined with enhanced wall treatment, it provided the most accurate predictions of airflow velocity distribution compared to other models. The study emphasizes that in enclosed and geometrically complex environments, such as vehicle or aircraft cabins, the SST k–ω model yields reliable and precise results.

Du et al. (2017) conducted experimental measurements of the jet flow field within an aircraft cabin mock-up, focusing on the impact of nozzle air supply temperature and volume flow rate on passengers' thermal sensations and perceptions of air movement. The study revealed that variations in nozzle air supply parameters significantly influence the airflow characteristics, which in turn affect passenger comfort levels. The study provides recommendations on the airflow rate from nozzles at different ambient temperatures.

Houghten et al. (1938) significantly contributed to the understanding of thermal comfort in the late 1930s. Their research investigated the role of temperature and air movement in influencing thermal comfort within various building environments, including offices, retail spaces, and transit stations. Additionally, Houghten et al. (1938) examined the discomfort caused by drafts experienced at sensitive areas, such as the back of the neck and ankles. Based on their findings, they emphasized that air-conditioning systems should be designed to ensure the absence of drafts for at least 90% of the occupants within a conditioned space. This landmark study laid the foundation for future work in the field of thermal comfort and HVAC system design.

Mboreha and colleagues (2021) employed Fanger's thermal comfort model to numerically analyze six distinct ventilation systems within the Boeing 767 aircraft cabin. The study identified the optimal individual ventilation system by considering factors such as the positioning of ventilation systems, air outlet temperature, and geometric parameters.

Maier et al. (2017) investigated the effect of ventilation types on thermal comfort in the passenger cabin of an aircraft. They examined the mixing ratio of the air inside the cabin with the air outside in different conditions. As a result, it was seen that the effect of ventilation types on thermal comfort is very little.

Zitek et al. (2010) studied the effect of personalized air outlets on passengers. The study showed that air outlets located in front of the passengers have a positive effect on the passengers. They concluded that the more outlets in front of the passengers, the higher the comfort.

Rydberg et al. (1949) introduced the concept of Effective Draft Temperature (EDT), which quantifies the temperature deviation of an air jet from its surrounding environment as a function of the jet velocity. This relationship provided a refined approach to assessing thermal comfort, as it accounts for the impact of localized air movement on perceived temperature. The introduction of EDT allowed for more accurate evaluations of how drafts affect occupant comfort, making it a valuable tool for improving HVAC system design and ensuring optimal thermal comfort in indoor environments.

Chun et al. (2004) argued that Fanger's PMV model is insufficient for accurately predicting thermal comfort in transitional spaces, which are characterized by unsteady and non-homogeneous conditions. They highlighted that the PMV model relies on the assumption of environmental homogeneity, which is not applicable in transitional spaces where local thermal sensation plays a more significant role than the overall body comfort. As a result, they suggested that alternative approaches are needed to assess thermal comfort in these types of environments, where localized factors, such as air movement and temperature variation, are more influential.

Madsen (1978) investigated the assessment of thermal comfort and discomfort based on the Effective Temperature (ET) parameter. By incorporating factors such as clothing insulation, mean radiant temperature, air velocity, and air temperature, he formulated an expression which was found to be consistent with the Predicted Mean Vote (PMV) index. The results of the study demonstrated that thermal comfort can be reliably represented using the ET.

According to the ISO 14505-3 (2006), unlike the Fanger model, which uses PMV and PPD to assess the overall condition of the human body, the equivalent temperature model can evaluate thermal comfort for different body parts.

Moon et al. (2016) conducted an investigation into the thermal comfort within an automobile cabin subjected to solar load, utilizing both the PMV and Equivalent Temperature (ET) models. They concluded that the PMV model was insufficient for evaluating localized variations in thermal comfort across different body parts, primarily due to its assumption of a homogeneous environment.

3. TURBULANCE MODELLING

In this chapter, the Reynolds averaging process is described, and the fundamental equations governing fluid flow and heat transfer are presented. The Boussinesq approach, which is one of the closure methods for the Reynolds-Averaged Navier-Stokes (RANS) equations, is discussed in detail along with the standard k-ε turbulence model and the near-wall treatment.

The Reynolds-Averaged Navier-Stokes (RANS) model is a widely used approach in CFD due to its efficiency in predicting turbulent flows while maintaining a reasonable computational cost. This model simplifies turbulence by decomposing instantaneous flow variables into their mean and fluctuating components, enabling a time-averaged representation of turbulent effects.

Different types of RANS models exist, with k-ε and k-ω being among the most common. The k-ε model is particularly effective for high-Reynolds-number flows, offering a reliable estimation of turbulence characteristics. Menter (1994) developed the k–ω SST (Shear Stress Transport) turbulence model to address the shortcomings of conventional models in accurately predicting flow separation. By combining the near-wall accuracy of the k–ω model with the free-stream robustness of the k–ε model, the SST formulation offers improved performance under adverse pressure gradient conditions. It has since become a widely used model in various engineering fields, particularly in aerospace and turbomachinery applications. In contrast, the k-ω model is more accurate near solid boundaries, making it well-suited for cases with significant boundary layer effects. In confined and complex internal flow geometries such as helicopter cabins, the k–ω SST turbulence model was selected due to its capability to accurately capture flow behavior near walls. This model offers reliable results in thermal comfort analyses thanks to its ability to simulate mixed convection conditions with higher precision.

3.1 Governing Equations:

In this section, the continuity equation, momentum equations, and turbulence equations related to the methods used are presented.

Equation 3.1 is the conservation equation of mass.

$$\frac{\partial \rho}{\partial t} + \frac{\partial}{\partial x_i}(\rho \bar{u}_i) = 0 \qquad (3.1)$$

where ρ is density of the fluid and $\bar{u}_i$ is the time average velocity.

Equation 3.2 is the momentum equation.

$$\frac{\partial \rho_m u}{\partial t} + \nabla \cdot (\rho_m u \vec{V}) = -\frac{\partial \mathrm{P}}{\partial x} + \nabla \cdot (\mu_m \nabla u) + \rho_m g_x + F_x \qquad (3.2)$$

$$\frac{\partial \rho_m v}{\partial t} + \nabla \cdot (\rho_m v \vec{V}) = -\frac{\partial \mathrm{P}}{\partial y} + \nabla \cdot (\mu_m \nabla v) + \rho_m g_y + F_y \qquad (3.3)$$

$$\frac{\partial \rho_m w}{\partial t} + \nabla \cdot (\rho_m w \vec{V}) = -\frac{\partial \mathrm{P}}{\partial z} + \nabla \cdot (\mu_m \nabla \mathrm{w}) + \rho_m g_z + F_z \qquad (3.4)$$

The Reynolds stress term and turbulent kinetic energy are calculated using the Boussinesq approximation.

$$-\rho_m \overline{V_i' V_j'} = \mu_T \left(\frac{\partial \bar{V}_i}{\partial x_j} + \frac{\partial \bar{V}_j}{\partial x_i} \right) - \frac{2}{3} m \delta_{ij} k \qquad (3.5)$$

$$k = \frac{1}{2} \overline{V_i' V_i'} \qquad (3.6)$$

Equation 3.7 is the turbulent kinetic energy equation in kω-SST equation.

$$\frac{\partial (\rho k)}{\partial t} + \frac{\partial (\rho u_j k)}{\partial x_j} = P_k - \beta^* \rho \omega k + \frac{\partial}{\partial x_j} \left[(\mu + \sigma_k \mu_t) \frac{\partial k}{\partial x_j} \right] \qquad (3.7)$$

$$P_k = \tau_{ij} \frac{\partial u_i}{\partial x_j} \qquad (3.8)$$

$$\mu_t = \frac{\rho a_1 k}{\max(a_1 \omega, S F_2)} \qquad (3.9)$$

Equation 3.10 is specific dissipation rate (ω) equation.

$$\frac{\partial(\rho\omega)}{\partial t}+\frac{\partial(\rho u_j\omega)}{\partial x_j} = \frac{\alpha\omega}{k}P_k-\beta\rho\omega^2+\frac{\partial}{\partial x_j}\left[(\mu+\sigma_\omega\mu_t)\frac{\partial\omega}{\partial x_j}\right] + 2(1-F_1)\rho\sigma_{\omega2}\frac{1}{\omega}\frac{\partial k}{\partial x_j}\frac{\partial\omega}{\partial x_j} \tag{3.10}$$

$$\mu_t=\frac{\rho k}{\omega}*\frac{1}{\max[\frac{1}{a^*},\frac{SF_2}{a_1\omega}]} \tag{3.11}$$

The constants of the k–ω SST model are adopted as shown in Equation (3.12).

$$a_1=0.31, \beta_1=0.075, \beta_2=0.0828, \sigma_{k1}=0.85, \tag{3.12}$$

$$\sigma_{k2}=1, \sigma\omega_1=0.5, \sigma\omega_2=0.856$$

4. MESH INDEPENDENCE STUDY

In this study, due to the difficulty and high cost of setting up the test environment for each case, the analyses conducted within the scope of the thesis have not been validated through testing. In this section, a study validated with both tests and analyses found in the literature is reviewed, and a mesh independence study is performed. The mesh structure obtained in this section has been used in the analyses carried out within the scope of this thesis.

For the mesh verification, the analysis results are evaluated using the experimental study conducted by Günther et al. (2006). In the research, a simplified cabin section, representing the area between the passenger seats and the overhead luggage compartments of a modern wide-body aircraft, as illustrated in Figure 4-1, is modeled. The analysis domain on the aircraft is illustrated in Figure 4.1.

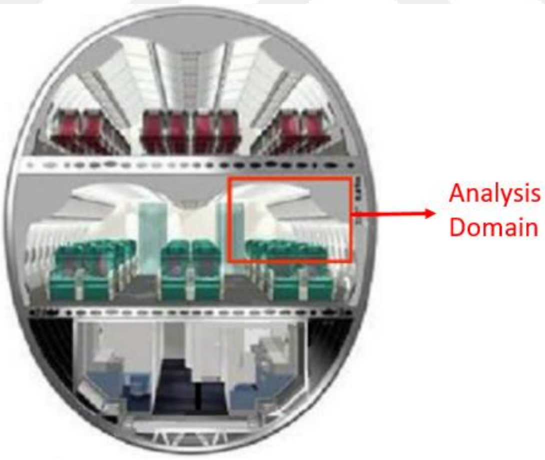

Figure 4.1 : Test and Analysis Domain

Since the overhead luggage compartment occupies a large area on the aircraft, a simplification is made in the test environment, and only a specific portion of the volume was included in the test. Thus, high costs were avoided both in setting up the test environment and in obtaining the test results. The luggage compartment volume used in the test is shown in Figure 4.2.

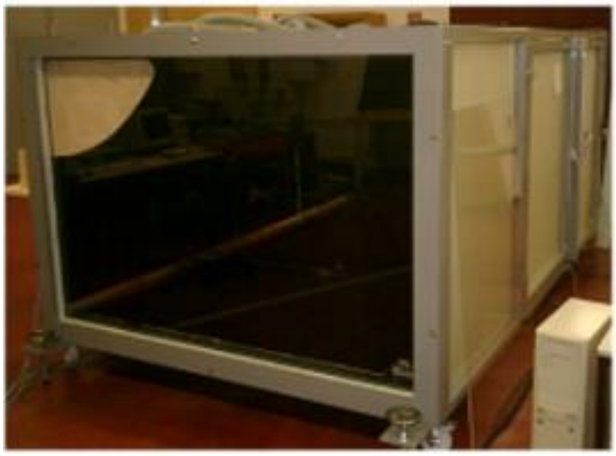

Figure 4.2 : Luggage Compartment Test Domain

Günther et al. (2006) compared the test results with simulation outcomes and provided recommendations for the appropriate turbulence model. Within the scope of this thesis, simulations were conducted using different mesh structures and compared with the experimental results.

To perform the simulations, the luggage compartment was simplified, and the flow domain is illustrated in Figure 4.3. In order to reduce the computational time and increase efficiency, the analyses were carried out using a portion of the total domain. The geometry used for the simulations is indicated in Figure 4.3.

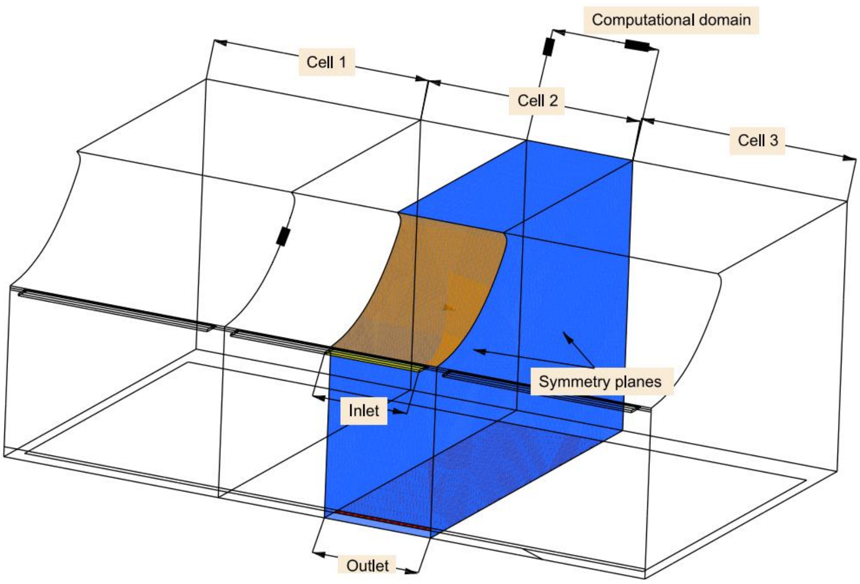

Figure 4.3 : CFD Analysis Domain

The names of the analysis boundaries and the dimensions of the analysis geometry are shown in Figure 4.4. To reduce the analysis time, symmetry boundary conditions are applied to the side walls of the geometry. In the conducted experimental study, velocity values were obtained using PIV along three different lines. The positions and coordinates of these lines are also presented in Figure 4.4.

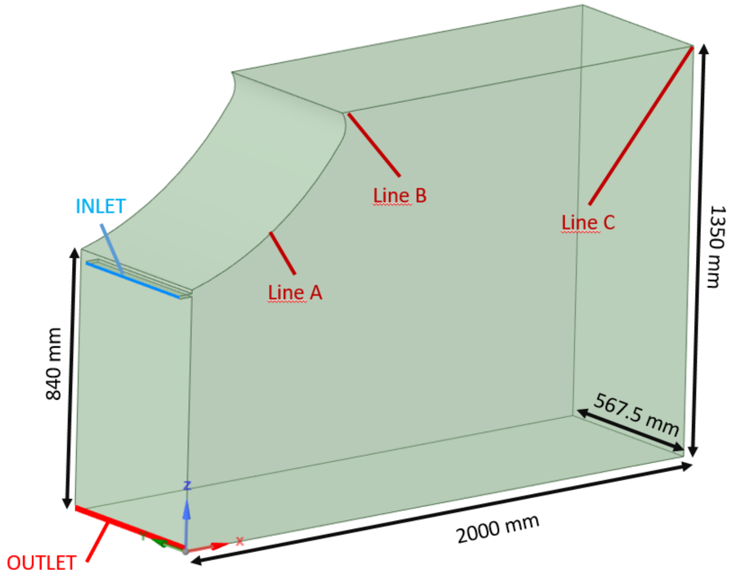

Figure 4.4 : CFD Analysis Geometry and Dimensions

The start and end coordinates of Line A, Line B, and Line C are given in Table 4.1. Velocity magnitude values are obtained at various positions along these lines.

Table 4.1 : Start and End Coordinates of Lines

Line		x	y	z
A	Start	357.5	0	961.7
	End	446	0	805
B	Start	682.7	0	1350
	End	868.9	0	1114.7
C	Start	2000	0	1350
	End	1434.3	0	784.3

Within the scope of this thesis study, the velocity data obtained along Lines A, B, and C were compared with the analysis results. The analyses were conducted using the widely used and validated k-ω SST turbulence model found in the literature. Table 4.2 provides the mesh configuration details created for mesh independence. Analyses are conducted using different mesh configurations to validate the method and perform a mesh independence study. The mesh structure was created by varying parameters such as mesh size, inflation rate, and first layer thickness, followed by the corresponding analyses. In all mesh studies, care was taken to keep the y+ value below 1, and the analyses were performed accordingly. As the mesh size and the number of inflation layers increase, the time required for the analysis also increases; however, the accuracy of the analysis can improve. With these mesh structures, the relationship between increased mesh count and improved accuracy has been investigated.

Table 4.2 : Mesh Information for Mesh Independence Study

		Mesh 1	Mesh 2	Mesh 3	Mesh 4	Mesh 5
Surface	Global Sizing	20 mm	20 mm	16 mm	12 mm	9 mm
	Outer Surfaces	15 mm	12 mm	11 mm	10 mm	8 mm
	Inlet & Outlet	4 mm	3.5 mm	3 mm	2.5 mm	2.5 mm
	Sharp Corner	2 mm	1.5 mm	1.2 mm	1.1 mm	0.9 mm
Inflation Layer	First Layer Thickness	0.4 mm	0.3 mm	0.2 mm	0.15 mm	0.15 mm
	Number of Layers	14	15	17	18	18
	Growth Layer	1.2	1.15	1.15	1.15	1.15
	Total Layer Thickness	22.6 mm	20.8 mm	19.6 mm	18.9 mm	18.9 mm

Analyses are conducted using the mesh structures provided in Table 4.2 and compared with the test results. In Figure 4.5, the values along Line A obtained from the test and simulation results are compared.

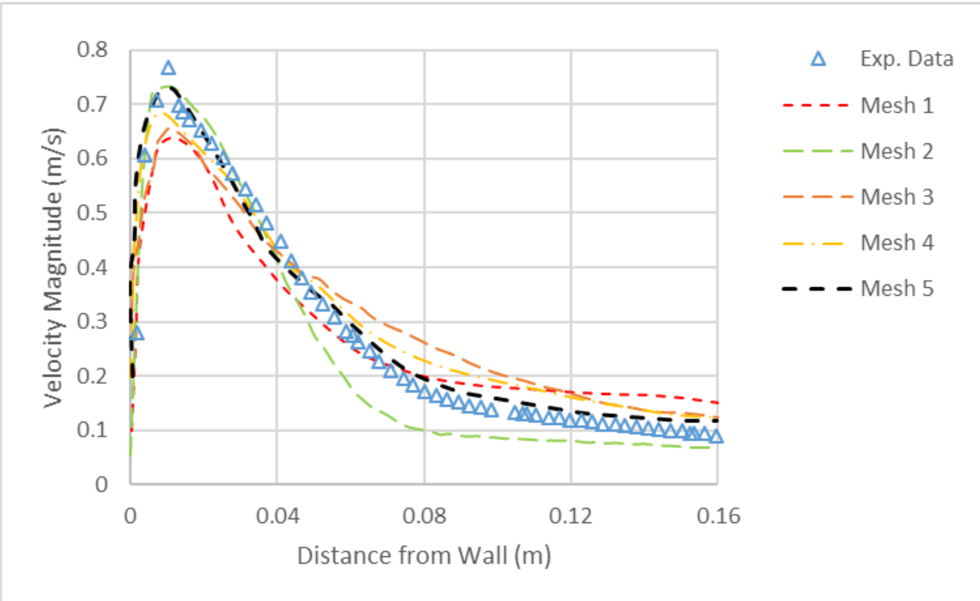

Figure 4.5 : Test and Analysis Results Comparasions for Line A

When the simulation results are compared with the test data, it is observed that all mesh types capture the general velocity magnitude trend. As the mesh is refined from

Mesh 1 to Mesh 5, the results show closer agreement with the experimental data. The comparison of velocity results obtained along Line B with the simulation results is presented in Figure 4.6.

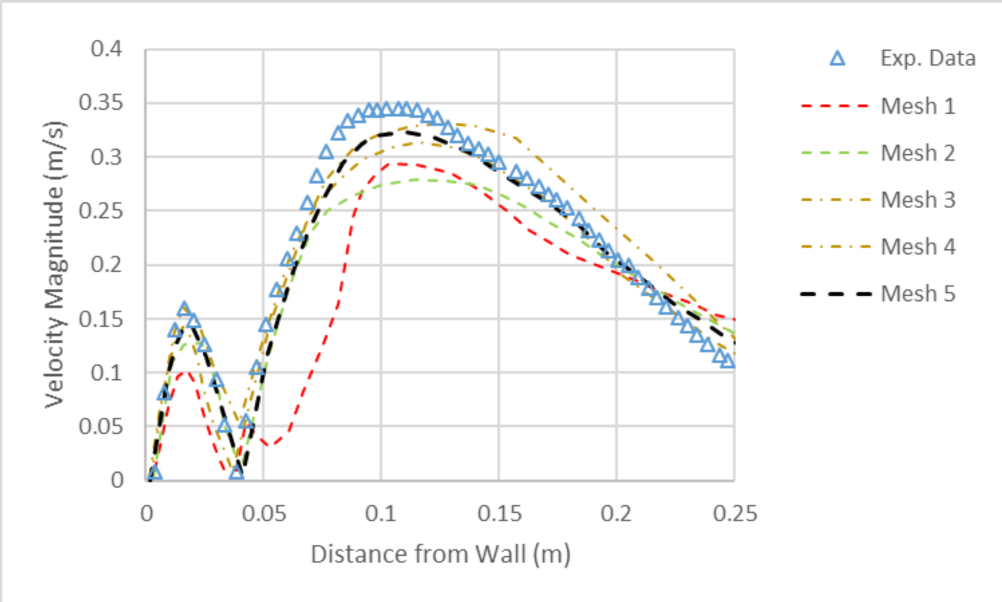

Figure 4.6 : Test and Analysis Results Comparasions for Line B

As observed for Line A, the increased mesh density also results in better agreement with the test data for Line B. In this case, the Mesh 5 structure provides more accurate resolution near the walls and in the internal regions, yielding results that are closer to the experimental data. The comparison of velocity magnitude values obtained along Line C between the simulation results and experimental data is presented in Figure 4.7.

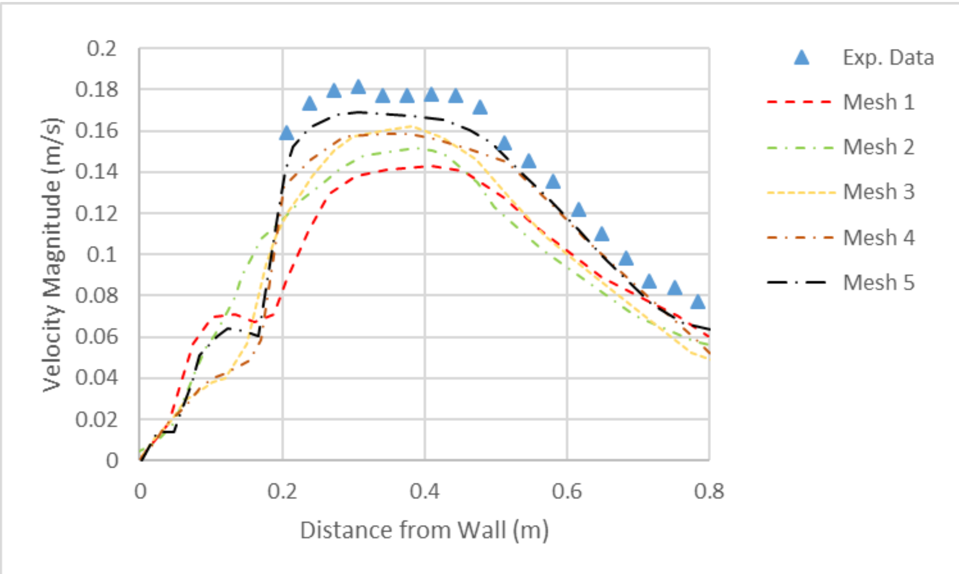

Figure 4.7 : Test and Analysis Results Comparasions for Line C

When the obtained simulation results and test data are evaluated together, it is observed that smaller mesh sizes near the wall region yield results that are closer to the experimental data. In this context, moving from Mesh 1 to Mesh 5, the number of mesh elements increases, and accordingly, the agreement with the test results improves. The y^+ values along the walls are presented in Figure 4.8. When the y^+ distribution is examined, it is observed to be below 1 on the walls.

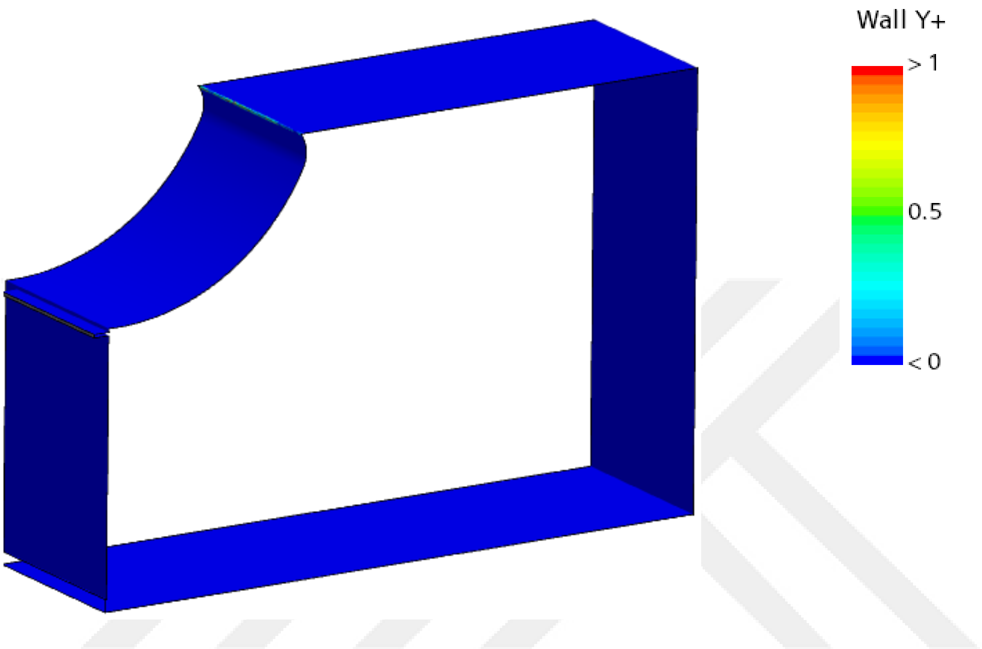

Figure 4.8 : y+ Distribution on the Walls.

When the results are examined, it is observed that the Mesh 5 configuration provides results that are in close agreement with the experimental data and successfully captures the overall trend. With this stage of the thesis, the turbulence model and mesh structure to be used have been validated. The thermal analyses for the helicopter are conducted using the knowledge and experience gained from this part of the study.

5. DEFINITION OF THERMAL COMFORT PARAMETERS

This section outlines the methodology and standards employed in the assessment of thermal comfort. The expressions and formulas defining thermal comfort have been presented with references to the literature and standards.

Thermal comfort in aircraft cabins has been discussed in various studies, but most findings are presented as recommendations rather than strict requirements. Still, taking these suggestions into account during the design phase can help improve passenger comfort. Certain standards offer guidance on airflow characteristics inside the cabin. For example, SAE ARP292 (2003) suggests that when individual air outlets (gasper nozzles) are used, the airflow velocity at seat level should be at least 200 ft/min (about 1 m/s). Similarly, ASHRAE (2013) recommends that air velocity at head level should exceed 1 m/s when personal ventilation is provided. ASHRAE (2007) also defines an acceptable range between 1 and 3 m/s in the head area under gasper operation. Regarding temperature distribution, SAE ARP292 (2003) advises that the vertical temperature difference from 5 cm above the floor to seated head height should not be greater than 5 °F (2.8 °C). However, the exact source and delivery conditions of the cabin air are not strictly defined in these standards, giving designers some flexibility. This study aims to contribute to this area by examining how airflow and ventilation setups affect thermal comfort inside the cabin.

Thermal comfort refers to a condition of mind in which a person expresses satisfaction with the thermal environment. It is influenced by a combination of environmental parameters such as air temperature, humidity, air velocity, and radiation, as well as personal factors like clothing insulation and metabolic rate. One of the most recognized approaches for evaluating thermal comfort is the model developed by P. O. Fanger in 1970, based on his extensive research on human thermal sensation and comfort (Fanger, 1970). Fanger's method combines both environmental and personal variables to calculate indices such as the PMV and PPD. The PMV index predicts the average thermal sensation of a large group of people on a scale ranging from cold to hot, while the PPD estimates the percentage of individuals likely to feel discomfort under those conditions. Fanger's model has been adopted in international standards, including ASHRAE Standard 55 (2017) and International Organization for Standardization (2005). However, due to the complexity of real environments, especially in confined and dynamic spaces like aircraft cabins, alternative approaches are also used. These include local thermal comfort metrics such as Equivalent Temperature (ET) and Effective Draft Temperature (EDT), which provide spatially resolved insights into perceived comfort. Such parameters are particularly valuable in computational fluid Dynamics based assessments where airflow distribution and local effects are critical. This study investigates thermal comfort through the analysis of ET and EDT, which are key indicators in evaluating local thermal conditions.

5.1 Fanger's Thermal Comfort Model

Fanger (1970) developed a mathematical model to evaluate thermal comfort, which includes six primary factors which are air temperature, radiation temperature, relative humidity, wind speed, clothing thermal resistance and activity. PMV is a calculation method used to predict the thermal comfort of an environment and is calculation is given Equation 5.1

$$\mathrm{PMV} = [0{,}303\mathrm{e}^{-0{,}036\,\mathrm{M}} + 0{,}028] * [\mathrm{T_a} - \mathrm{T_r}) + 0{,}92(\mathrm{M} - \mathrm{W})] \quad (5.1)$$

In the Equation 5.1, several parameters are considered to evaluate thermal comfort. These include the air temperature ($\mathrm{T_a}$), the mean radiant temperature ($\mathrm{T_r}$), metabolic heat generation (M, expressed in $\frac{\mathrm{W}}{\mathrm{m^2}}$), and the external work performed by the individual (W). Each of these variables plays a significant role in determining the thermal sensation experienced by an passangers.

PPD estimates the percentage of people likely to feel dissatisfied based on the PMV. Equation 5.2 is the calculation of PPD.

$$PPD = 100 - 95 * e^{-0{,}03353*PMV^4 - 0{,}2179*PMV^2} \quad (5.2)$$

Equation 5.2 shows the relationship between PMV and PPD, where a higher PMV (either positive or negative) results in a higher percentage of dissatisfied people. Even at PMV = 0 (optimal thermal comfort), PPD is typically around 5%, indicating that some level of dissatisfaction is always present due to individual differences. Figure 5.1 illustrates the relationship between PMV and PPD.

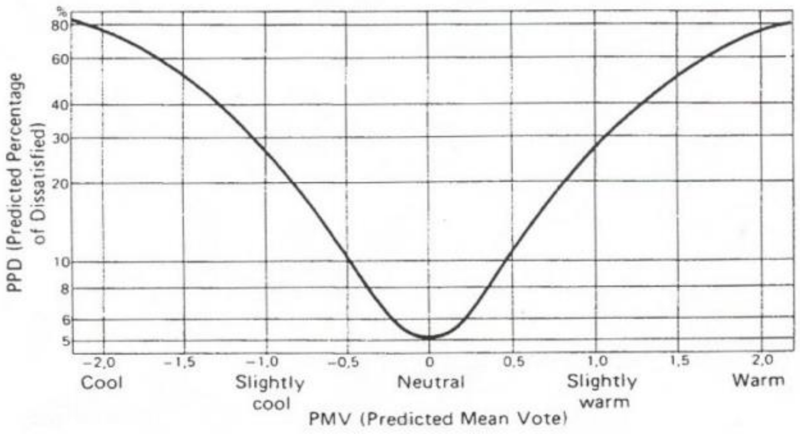

Figure 5.1 : PMV and PPD Graph.

5.2 Equivalent Temperature

Equivalent Temperature (ET) is based on thermal comfort studies that have been conducted since the 1950s. It is primarily developed through empirical models created by organizations like Fanger (1970) and ASHRAE (2017), which are designed to measure and assess thermal comfort.

Fanger's PMV model is one of the first comprehensive frameworks for evaluating thermal comfort, aiming to understand how environmental factors (such as temperature, air velocity, humidity, etc.) impact human comfort. However, while the PMV model focused more on factors like relative temperature and humidity, the ET model combines a broader set of parameters, including not only air temperature but also radiation, air velocity, and clothing insulation, providing a more comprehensive representation of thermal perception.

The Equivalent Temperature formulation has been progressively refined based on established thermophysiological and environmental principles to enable a more systematic and generalizable assessment of the combined effects of all modes of heat exchange in an environment. This approach seeks to enhance the accuracy of thermal comfort evaluation across a wide range of environmental conditions. Equation 5.2 represents the empirical expression employed for the calculation of Equivalent Temperature.

$$ET = 0.55T_a + 0.45MRT + \frac{0.24 - 0.75\sqrt{v}}{1 + I_{cl}}(36.5 - T_a) \quad (5.3)$$

$$For\ v > 0.1\ m/s$$

$$ET = 0.5(MRT + T_a) \quad (5.4)$$

$$For\ v < 0.1\ m/s$$

where T_a is the air temperature in degree Celcius, v is air velocity (m/s) and I_{cl} is clothing insulation.

$$MRT = \Sigma_n F_{p-i} \times (T_i) \quad (5.5)$$

In Equation 5.4, MRT represents the mean radiant temperature in degrees Celsius. The term F_{p-i} refers to the view factor between the person and the i^{th} surface, while n denotes the total number of surfaces considered. T_i represents the temperature of any given surface, measured in degrees Celsius.

I_{cl} is the clothing insulation unit that measures the heat insulation capacity of the clothing worn and its unit is clo. Since the heat insulation created by each garment to the body is different, I_{cl} values also differ from each other. I_{cl} depends on the material type, thickness and length of the clothing. 1 clo is defined as the clothing combination that allows a person to feel comfortable in an enclosed space at a temperature of 21 °C. Some clothes and their clo values are given in Table 1.

Table 5.1 : Clothes and Clothing Isolations.

Clothes	I_{cl} (clo)
T-shirt	0.10-0.15
Long Sleeved Shirt	0.25
Jeans	0.30
Fabric Trousers	0.25
Boots	0.20-0.25
Casual Shoes	0.03
Light summer outfit (T-shirt + shorts + sandals)	0.30-0.35
Office outfit	0.85-1.00
Winter clothes	1.50-2.00

5.3 Effective Draft Temperature

Effective Draft Temperature (EDT) is a measure used to quantify the local sensation of warmth or coolness. It represents the temperature difference resulting from the combined effects of air temperature and airspeed. EDT is determined by two key factors: the first is the difference between the local air temperature (T_a) and the room control temperature (T_c), and the second is the airspeed (v). These two factors together influence an individual's thermal comfort. In this equation, T_c refers to the fixed average room temperature, and according to the ASHRAE (2017), a reference value of T_c = 24.5 °C is used to evaluate the deviation of local air temperature when calculating EDT. Equation 5.6 is emprical relation for Equivalent Temperature.

$$EDT = (T_a - T_c) - 0.1276(v - 0.15) \tag{5.6}$$

where T_a is the air temperature in degree Celcius, T_c is the average room temperature in degree Celcius and v is air velocity ($\frac{\mathrm{m}}{\mathrm{s}}$).

The acceptable limits for EDT are defined in the standards. For individuals to feel comfortable, the EDT value should range between -1.7°C and 1.1°C. If the EDT exceeds 1.1°C, it is considered hot, while if it falls below -1.7°C, it is considered cold. EDT is used to assess how air movement, particularly at low speeds, affects the temperature sensation perceived by a person in the environment.

In this study, the thermal comfort of passengers is examined region by region, and evaluations are carried out accordingly. Although the Fanger method is more frequently used in the literature and standards due to its widespread application, it presents a coarse approach. The Fanger method does not allow for a region-based analysis of the passenger. Since the Fanger method treats the passenger as a whole, it is not considered sufficient for the purposes of this study. Therefore, the thermal comfort assessments are conducted based on ET and EDT parameters. In the analyses conducted throughout the thesis, it is assumed that passengers wear the same clothing. It is assumed that passengers wear a shirt and trousers, and casual shoes as footwear. Information regarding the clothing is given in Table 5.1. These values are assigned to the relevant regions, and the analyses are carried out accordingly.

6. THERMAL COMFORT INVESTIGATION FOR PASSANGERS IN HELICOPTER CABIN

In this chapter, the parameters affecting the thermal comfort of passengers inside the helicopter cabin are examined. The primary parameters influencing thermal comfort include the ambient air temperature, the velocity and temperature of the air directed toward the passengers, the angle of solar radiation incidence, the passengers' level of physical activity, and the thermal insulation values of their clothing. In the following sections, the parameters affecting thermal comfort are examined sequentially.

6.1 Description of Helicopter CFD Analysis Model

There are four passengers inside the helicopter cabin. The passengers are seated in two rows, facing each other, with two passengers in each row. The passengers are seated in their seats. The passengers and seats have been modeled to be identical to each other. The interaction between the passenger and the seat has not been modeled in the analysis. Cold air is supplied to the helicopter cabin through main outlets and air outlets, called gaspers, positioned for each passenger. There are four gaspers and two main outlets inside the cabin. The main outlets cannot be closed or adjusted by the passengers, whereas the gaspers can be adjusted by the passengers in terms of airflow rate and direction. When the gaspers are in the default position, they blow air directly downward. While the main outlets do not directly affect the thermal comfort of the passengers, the gaspers have a direct impact on comfort. The extent to which the gaspers affect comfort is examined in the subsequent sections of the study. The gaspers are positioned above each passenger, while the main air outlets are located equidistan from the seats. It is assumed that the air supplied from both the gaspers and the main air outlets is at the same temperature. In this study, the gasper and main air outlet ducts, as well as the pressure losses occurring within these ducts, are neglected. The cabin geometry, passengers, and seats are simplified in a manner that would not affect the accuracy of the analysis results. The simplified helicopter cabin geometry, along with the gaspers, main air outlets, passengers, and seats, is illustrated in Figure 1. Passengers are represented in orange, seats in green, and the lower cabin surface on which the passengers and seats are positioned is shown in black. In complex geometries such as helicopter cabins, the air inlet regions can be clearly defined, whereas determining the air outlet regions is considerably more challenging. This is because air may exit from any surface or region within the cabin. Therefore, in the analyses, cold air is supplied into the cabin through the gaspers and main outlets, while the air outlets are modeled as leakage surface. The modeled air outlet surface and cabin dimensions are all illustrated in Figure 6.1.

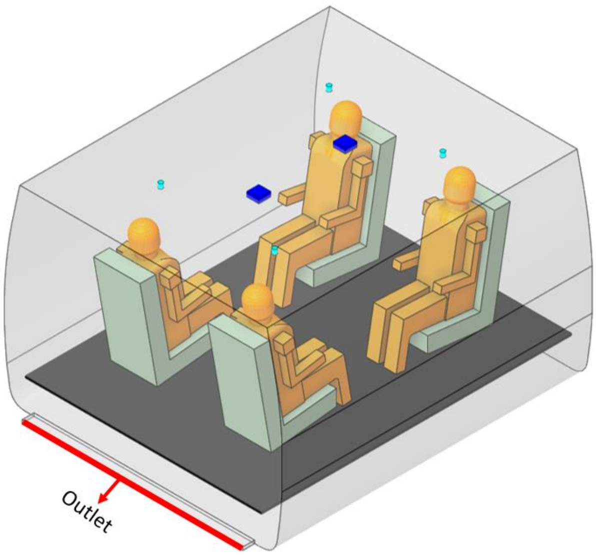

Figure 6.1 : Helicopter Cabin Fluid Domain CFD Geometry.

The geometry of the cabin and passengers from the side view is shown in Figure 6.2, while the rear view is illustrated in Figure 6.3.

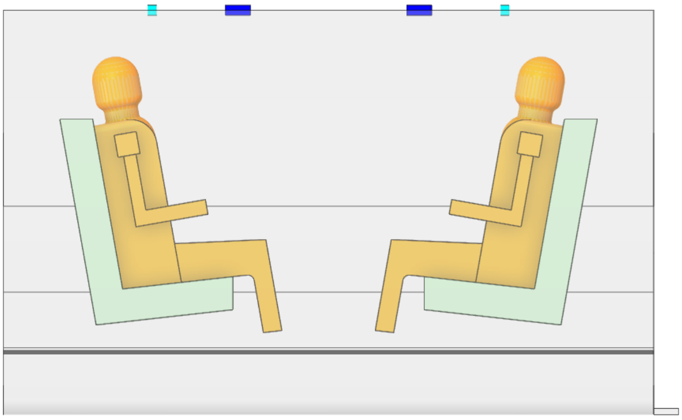

Figure 6.2 : Helicopter Cabin Geometry Side View.

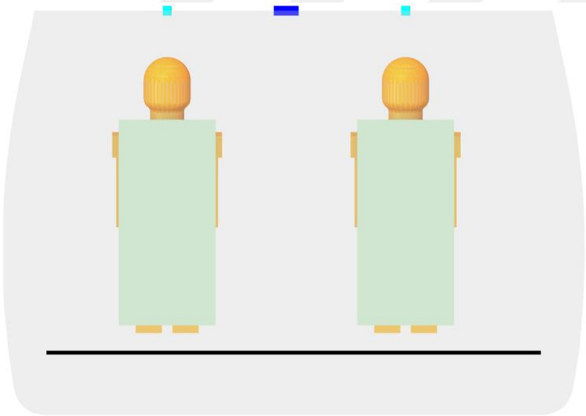

Figure 6.3 : Helicopter Cabin Geometry Back View.

In addition to the helicopter cabin flow geometry, a solid structure with a thickness of 5 mm is included to represent the structural parts of the cabin. The structure of helicopter cabin is illustrated in Figure 6.4.

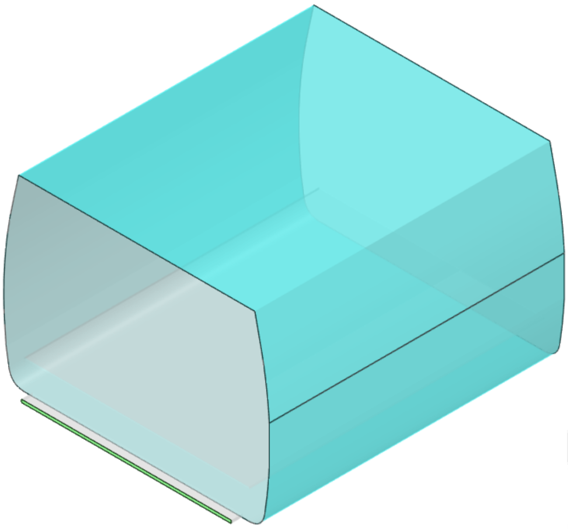

Figure 6.4 : Helicopter Cabin Solid Geometry.

Miracle et al (2001) identified the materials and physical properties assigned to the solid parts in the analyses, as presented in Table 6.1.

Table 6.1 : Materials and Physical Properties.

Surfaces	**Materials**	**Density (kg/m^3)**	**Spesific Heat (J/kg-K)**	**Thermal Conductivity (W/m-K)**
Shell	CFRP	1550	850	0.7
Seat	Polyurethane	70	1685	0.05
Floor	Aluminum Alloy	2700	900	167

According to ISO (2005) and various studies in the literature, the acceptable range for Equivalent Temperature (ET) to ensure thermal comfort typically lies between 22 °C and 27 °C. Maintaining ET values within this range helps occupants perceive the environment as thermally neutral, avoiding sensations of either excessive warmth or coolness. There are defined threshold values for acceptable Effective Draft Temperature (EDT) to maintain occupant comfort. When EDT values deviate from this acceptable range, thermal discomfort may occur. Comfort is generally maintained when EDT remains between -1.7 °C and 1.1 °C. EDT values exceeding 1.1 °C indicate a sensation of excessive warmth, while values below -1.7 °C are perceived as overly cool. To examine the thermal comfort of passengers in different scenarios, the body parts of the passengers have been considered separately. The head, shoulders, right arm, left arm, torso, right leg, and left leg regions are shown in different colors in Figure 6.5. In the analyses, the average ET and EDT temperatures are examined separately for each region.

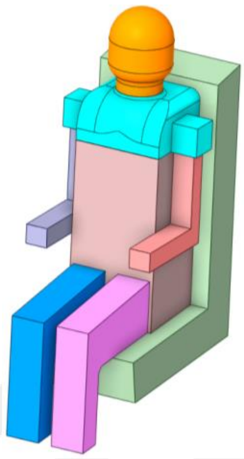

Figure 6.5 : Passenger Body Segment and Seat.

6.2 Development of CFD Model

In this study, the analysis of the parameters has been conducted using CFD simulations with the Star CCM+ software. Due to the high cost of conducting experimental tests and limited infrastructure, the study has been analyzed numerically. The boundary conditions used in the analyses are detailed in this section. Parameters influencing passenger thermal comfort such as the velocity and temperature of the air supplied through gaspers and main outlets, as well as the ambient temperature, are varied throughout the scenarios. In contrast, passenger metabolic heat load, heat gain from south-facing surfaces, and the solar incidence angle are kept constant. A velocity inlet condition is applied perpendicular to the surface, while a static pressure outlet with 0 Pa gauge pressure is defined for the outlet boundaries. Surfaces of the cabin geometry that are not in direct contact with the external environment were treated as adiabatic walls, and no-slip boundary conditions are applied to all solid surfaces except inlets and outlets. All simulations are conducted for the on-ground condition, which represents the thermally most challenging scenario for the helicopter. Zhang et al. (2008) demonstrated that a heat flux boundary condition can be uniformly applied to all faces and body surfaces of each passenger to ensure that the passenger heat load value. SAE (2011) defined the calculation of the external convective heat transfer coefficient as a function of airspeed under ambient conditions. The external air temperature is varied according to different cases, while the heat transfer coefficient is 10 W/m²K, with the helicopter considered to be in a stationary environment. Heat transfer coefficient can be expressed as Equation 6.1. h is the heat transfer coefficient ($\frac{W}{m^2K}$) and v is the wind speed ($\frac{m}{s}$).

$$h = 0.6 + 6.64\sqrt{v} \tag{6.1}$$

The temperature of the cooling air supplied to the cabin is adjusted based on varying cases. Additionally, the airflow velocities of each gasper and main air outlet are modified according to different scenarios. A solar heat load of 800 W/m² is applied, assuming the sun is positioned directly above the helicopter. The passenger heat load is set at 75 W. Various insulation coefficients are assigned to the clothing regions worn by each passenger, which are incorporated into the ET equation to account for thermal comfort.

In this study, the thermal comfort conditions of passengers are analyzed by examining the variation of specific parameters. The parameters investigated include: the position of the gaspers, the ratio of the gasper airflow rate to the main outlet airflow rate, the effect of changes in the gasper area on thermal comfort, and the relationship between the ambient air temperature and the supplied cold air temperature. In the following sections, each of these parameters are examined individually to assess their respective impacts on thermal comfort.

6.3 Mesh Independence Study

Before examining the parameters affecting the thermal comfort of passengers inside the helicopter, the suitability and mesh independence of the selected mesh structure must be evaluated. Since no experimental study is conducted within the scope of this thesis, it is necessary to demonstrate that the solution is independent of the mesh structure and size. In this context, using the boundary conditions specified in Section 6.4, simulations for Case 1 are carried out with different mesh structures and sizes. The k–ω SST turbulence model is employed, and analyses are conducted using four different mesh configurations, which are then compared with each other. The mesh structure details used for this purpose are provided in Table 6.2.

Table 6.2 : Mesh Informations for Mesh Independence Study for Helicopter Cabin Analyses.

		Mesh 1	Mesh 2	Mesh 3	Mesh 4	Mesh 5
Surface	Global Sizing	20 mm	16 mm	12 mm	10 mm	9 mm
	Outer Surfaces	15 mm	12 mm	9 mm	8 mm	7 mm
	Inlets & Outlet	3 mm	2.5 mm	2 mm	1.5 mm	1.3 mm
	Passengers Body & Seats	8 mm	6 mm	4 mm	3 mm	2.5 mm
Inflation Layer	First Layer Thickness	0.35 mm	0.35 mm	0.35 mm	0.35 mm	0.35 mm
	Number of Layers	10	10	10	10	10
	Growth Layer	1.2	1.2	1.15	1.15	1.15
	Total Layer Thickness	9.08 mm	9.08 mm	9.08 mm	9.08 mm	9.08 mm

This study initially considered applying different mesh sizes to various regions of the passengers. However, since the y^+ values observed on the passenger surfaces were found to be below 1, a uniform mesh size was applied to all regions of the passengers. The y^+ distribution on the passenger surfaces is shown in Figure 6.6.

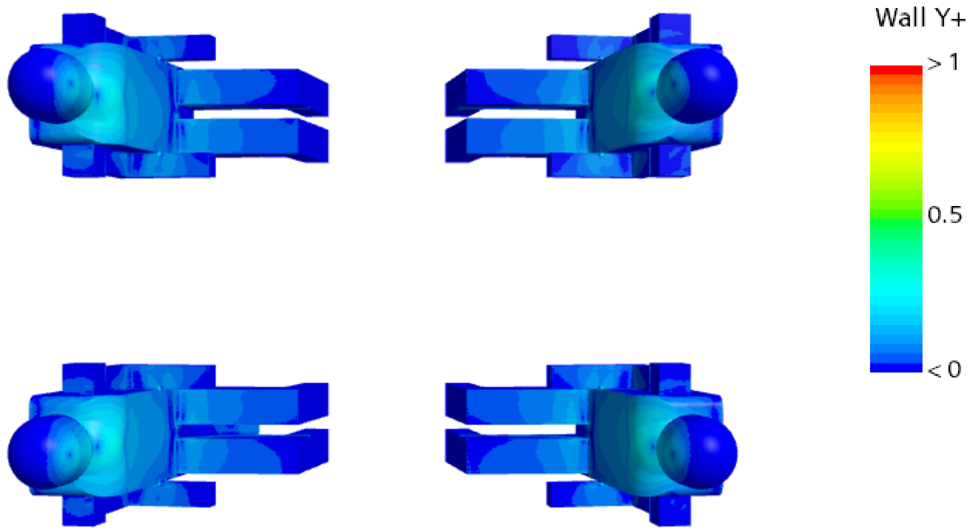

Figure 6.6 : y+ Distribution on Passangers.

It is known that the quality of the applied mesh significantly affects both the convergence of the solution and the accuracy of the results. Table 6.3 presents the applied mesh configurations along with their quality characteristics. A hexagonal mesh structure is used for analyses.

Table 6.3 : Mesh Properties for Mesh Independence Study.

	Mesh 1	Mesh 2	Mesh 3	Mesh 4	Mesh 5
Number of Elements	1882000	2476300	3744500	4578000	5348100
Maximum Skewness	0.82	0.81	0.79	0.79	0.77
Average Skewness	0.24	0.21	0.18	0.17	0.16
Average Cell Quality	0.78	0.81	0.85	0.86	0.85
Maximum Aspect Ratio	2.1	1.9	1.8	1.6	1.5

To demonstrate the accuracy of the mesh used, Case 1 analyses are conducted for all five mesh structures. In this context, the velocity magnitude values along the line from the floor to the main outlet are shown in Figure 6.7. The coordinates of Line A and Line B are given in Table 6.4.

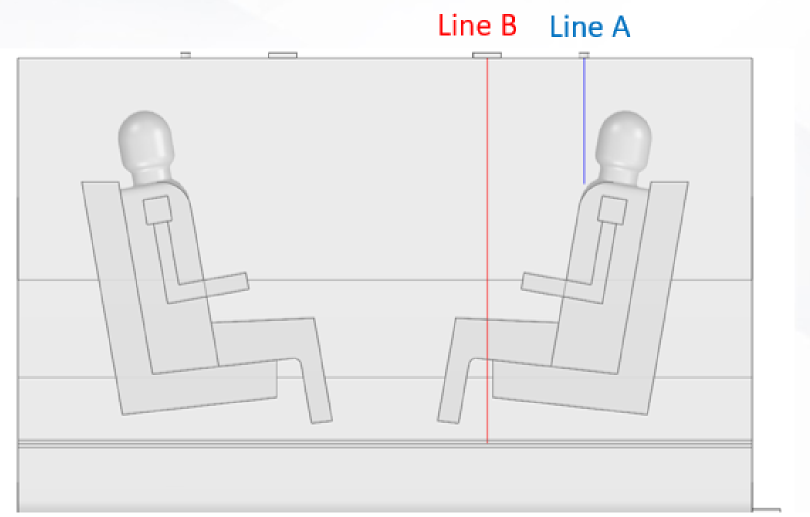

Figure 6.7 : Mesh Independence Study – Line A and Line B

Table 6.4 : Coordinates of Line A and Line B

Line		**x**	**y**	**z**
A	Start	3724	802	2317
	End	3724	357	2317
B	Start	4202	802	1974
	End	4202	-560	1974

Temperature and velocity distribution along Line A are shown in Figure 6.8 and Figure 6.9. Temperature and velocity distribution along Line B are shown in Figure 6.10 and Figure 6.11.

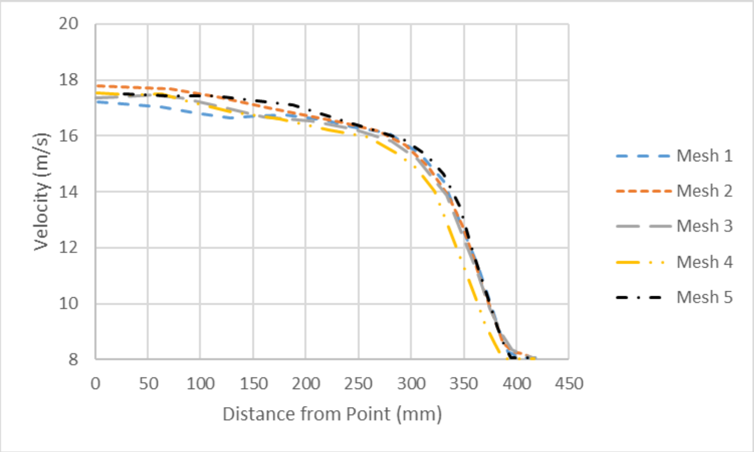

Figure 6.8 : Temperature Distribution along Line A

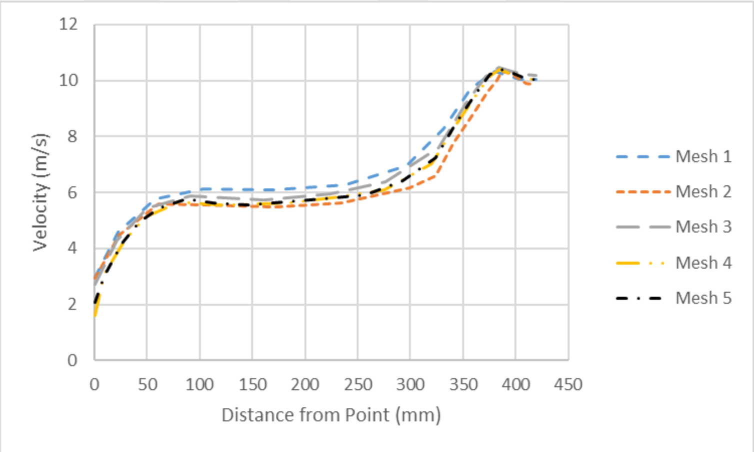

Figure 6.9 : Velocity Distribution along Line A

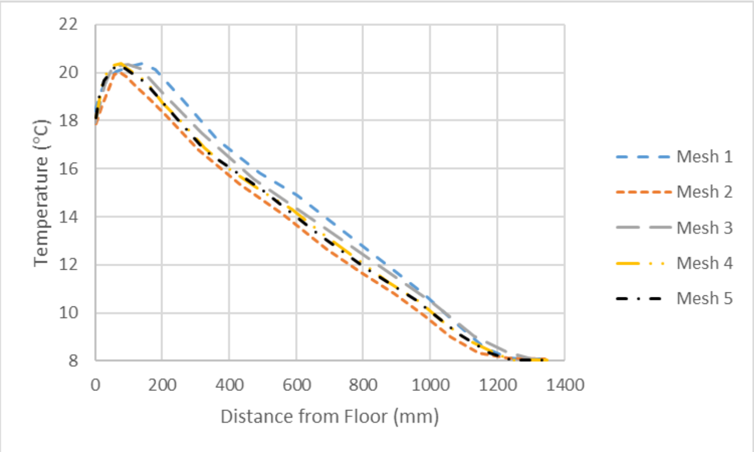

Figure 6.10 : Temperature Distribution along Line B

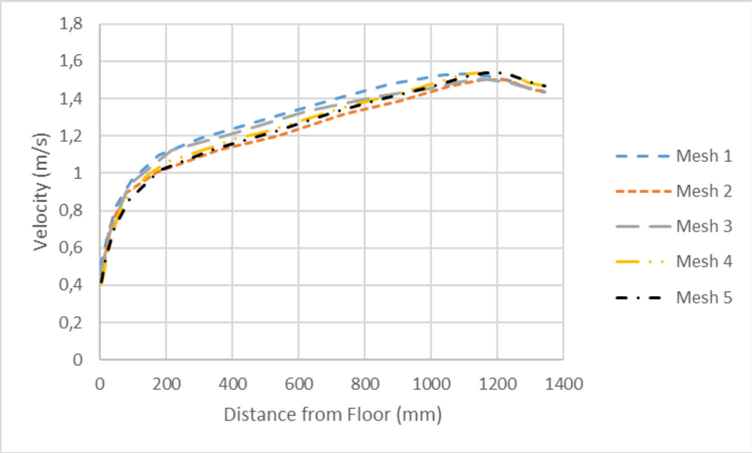

Figure 6.11: Velocity Distribution along Line B

When the analysis results conducted on different mesh structures are examined, it is observed that all meshes capture a similar velocity trend. The analyses with Mesh 4 and Mesh 5 structures are in good agreement. Considering both solution time and efficiency, Mesh 4 is selected for the analyses.

Figure 6.12 shows the variation of velocity magnitude at three different points over iterations in the analysis conducted with Mesh 4. It is observed that the changes in velocity values over iterations are negligible, indicating that the solution has converged.

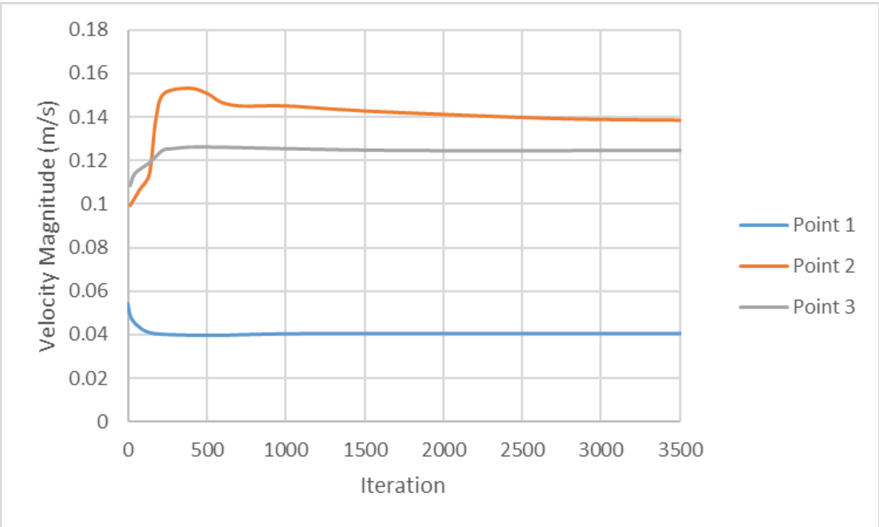

Figure 6.12 : Changing Velocity Magnitude of Points by Iteration

6.4 Investigation of the Effect of Gasper Position on Passanger Thermal Comfort

One of the key parameters influencing passengers' thermal comfort is the positioning of the gaspers. To analyze the investigated parameters in a more organized and effective manner, it is crucial to optimize the positioning of the gaspers. In this study, the gaspers are placed on the upper deck of the helicopter, directly above the passengers' heads. The literature and standards do not provide specific recommendations regarding the placement of gaspers. Therefore, it is appropriate to first determine an optimal gasper position before examining other parameters. The variations in gasper air inlet velocity and the supplied air temperature depend on the parameter being examined. The corresponding changes in boundary conditions are provided in the respective sections. The boundary conditions and assumptions for the analysis are given Table 6.5.

Table 6.5 : Boundary Conditions and Assumptions for Analyses

Outside	Temperature (°C)	50
	Convective Heat Transfer Coefficient (W/m^2K)	10
	Surface Emissivity	0,8
	Surface Transmissivity	0,2
	Surface Reflectivity	0
Main Air Inlet	Velocity (m/s)	1.5
	Temperature (°C)	8
Gasper Inlet	Velocity (m/s)	10
	Temperature (°C)	8
Outlet	Pressure (Pa)	$P_{staticgage} = 0$
Wall	Adiabatic	Between cabin and cockpit
Solar Load	Heat Flux (W/m^2)	800
Passenger	Heat Generation Rate (W)	75

In order to investigate the effect of gasper position on thermal comfort, the positions of the gaspers above each passenger are altered with the aim of determining the optimal gasper position. In the initial stage of determining the gasper position, it is necessary to define its distance from the passenger’s head, ensuring that it is aligned symmetrically with the passenger. In this regard, thermal comfort analysis is conducted for six different gasper positions. The positions and numbering of the gaspers are shown in Figure 6.13. The gasper locations information are given in Table 6.6.

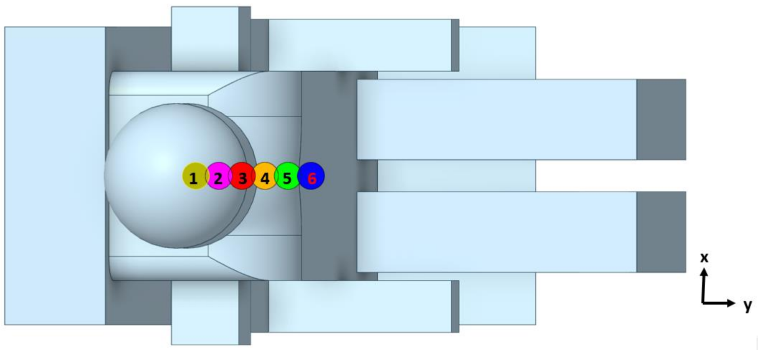

Figure 6.13 : Gasper Locations for Case 1-6.

Table 6.6: Gasper Positions and Locations for Case 1-6.

CASES	GASPERS	Distance from Referance Gasper Location in x-direction (mm)	Distance from Referance Gasper Location in y-direction (mm)
Case 1	G1	0	0
Case 2	G2	0	30
Case 3	G3	0	60
Case 4	G4	0	90
Case 5	G5	0	120
Case 6	G6	0	150

While analyzing the effects of the parameters on passengers' thermal comfort, the condition of each individual passenger is examined. The results of ET and EDT temperatures at the reference gasper location for all passengers are presented in Figure 5. P1 represents Passenger 1, P2 represents Passenger 2, P3 represents Passenger 3, and P4 represents Passenger 4. Figure 6.14 shows the labeling of passengers from a top view.

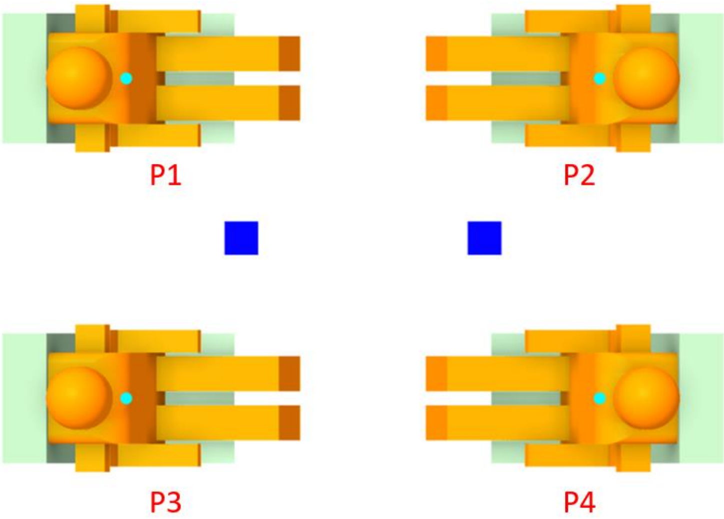

Figure 6.14 : Passenger Labeling and Top View of Passengers.

The evaluation of thermal comfort results across different cases investigates whether it is necessary to assess each passenger individually. In Figure 6.15 and Figure 6.16, the regional ET and EDT temperature values for each passenger in Case 1 are presented, respectively.

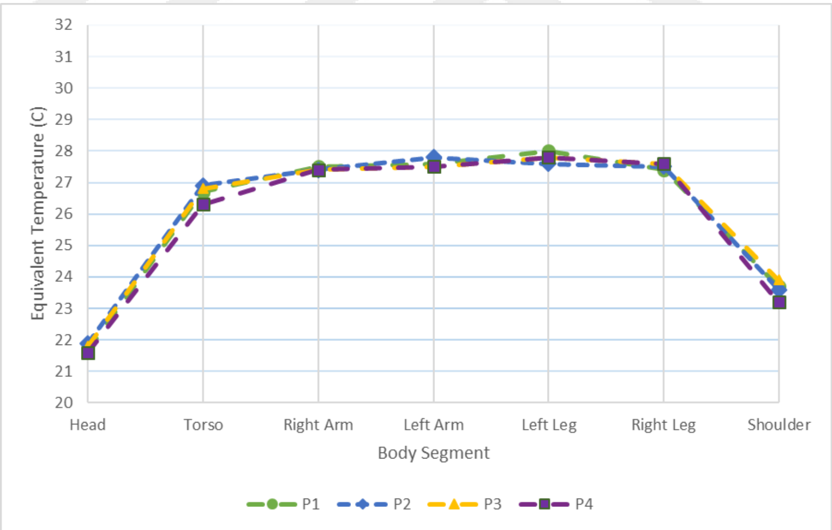

Figure 6.15 : Average ET Temperatures of Body Segement for Case 1.

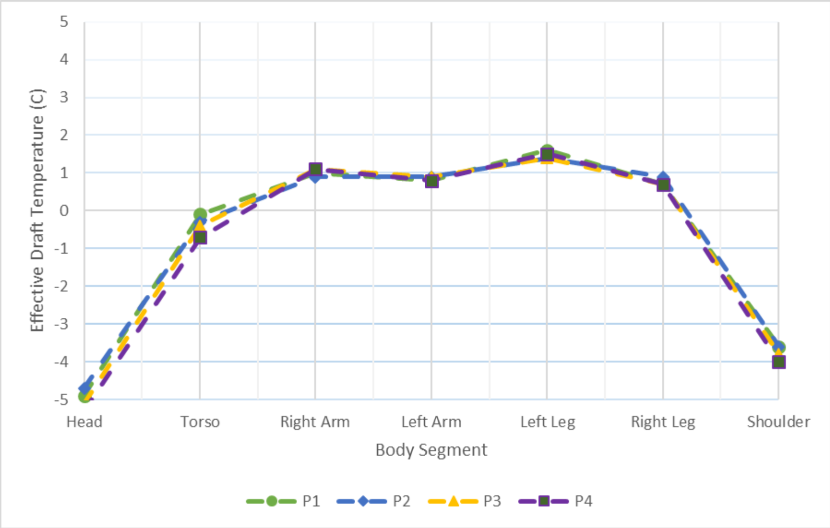

Figure 6.16 : Average EDT Temperatures of Body Segement for Case 1.

Upon examining the Case 1 analysis results, it is observed that separate thermal comfort analyses for Passenger 1, Passenger 2, Passenger 3, and Passenger 4 are not necessary. Similar results regarding thermal comfort are obtained for each passenger. Therefore, the thermal comfort analysis, including this parameter, has been conducted solely for Passenger 1 by examining the relevant regions of the passenger. The thermal comfort parameters obtained for the passengers exhibited a high degree of similarity. Therefore, in the evaluation of all other parameters, interpretations are based on the average surface temperature values of ET and EDT for Passenger 1.

To better examine the effect of gasper positions on thermal comfort, the analysis results from Cases 1 to 6 are evaluated collectively. For Passenger 1, the average ET and EDT temperature values by body region are presented in Figure 6.17 and Figure 6.18, respectively.

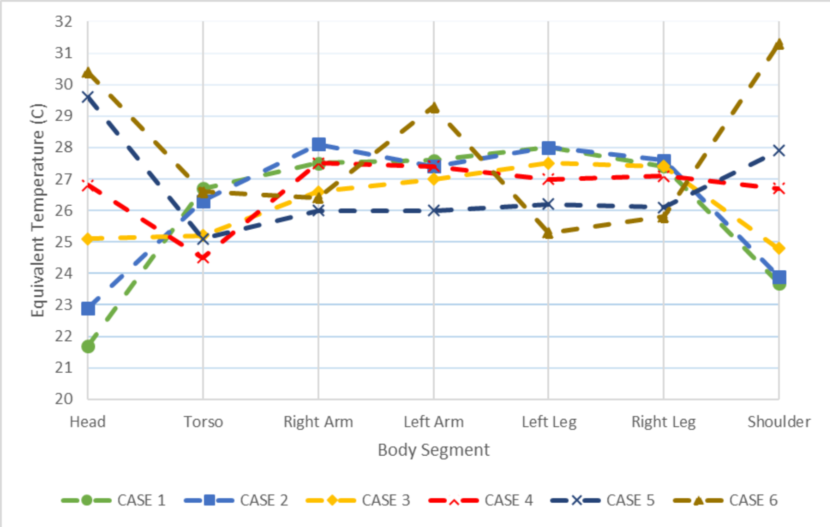

Figure 6.17 : Average ET Temperatures of Body Segement for Case 1-6.

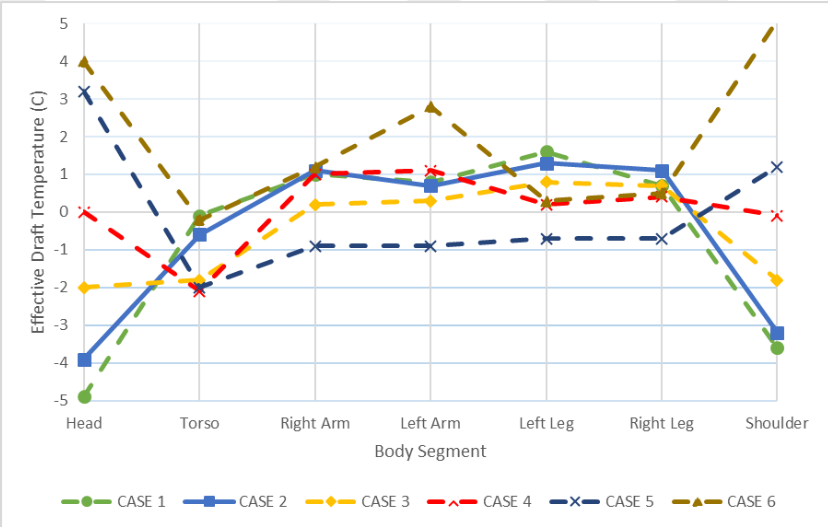

Figure 6.18 : Average EDT Temperatures of Body Segement for Case 1-6.

Upon evaluating the analysis results, it has been determined that the positions of the gaspers, symmetrically located above the passengers' heads, have a significant impact on thermal comfort. In the Case 1 scenario, the ET and EDT parameters clearly indicate that thermal comfort in the head and shoulder regions is negatively affected. The EDT temperatures in these regions fall below the acceptable threshold of -1.7 °C. Similar trends are observed in Case 2 and Case 3 gasper configurations. In contrast, the Case 4 gasper location yields average ET and EDT values in the head and shoulder regions that remain within acceptable ranges, providing a more balanced thermal comfort distribution. In Case 5 and Case 6, as the gaspers are positioned farther from the head area, a decrease in thermal comfort is observed in the head and shoulder regions, while other body areas show minimal variation in comfort compared to other scenarios. Based on these findings, the Case 4 gasper configuration will be used as a reference in the subsequent analysis set, which aims to examine the effects of varying gasper positions relative to the cabin's symmetry axis.

Figure 6.19, Figure 6.20, Figure 6.21, Figure 6.22, Figure 6.23, Figure 6.24 present the ET temperature distributions on the passengers' bodies, while Figure 6.25, Figure 6.26, Figure 6.27, Figure 6.28, Figure 6.29, Figure 6.30 illustrate the EDT temperature contours. The variations in these parameters according to gasper location are clearly visible. When the gasper is positioned directly above the head, the head and shoulder regions are negatively affected in terms of thermal comfort and tend to feel cold. As the gasper moves further from the head, thermal comfort is again negatively impacted, with those regions tending to feel warm. Considering these changes, it is important to carefully determine the placement of the gasper.

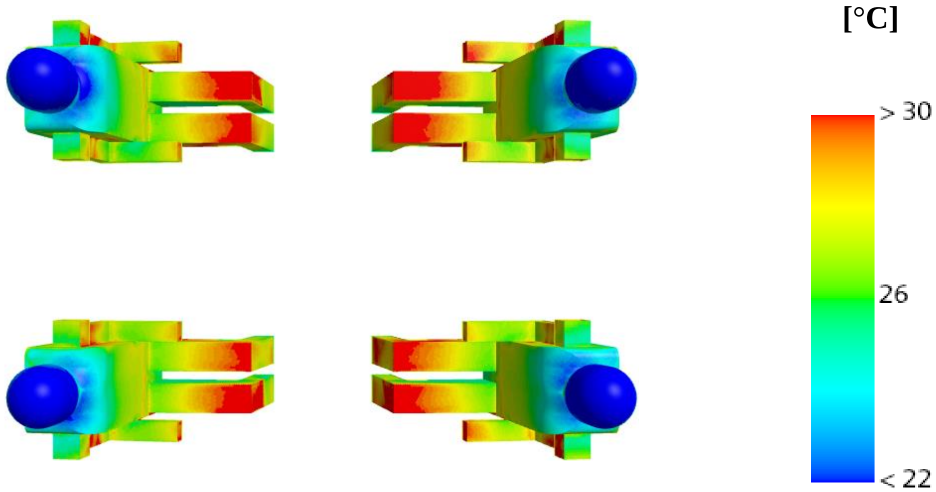

Figure 6.19 : Case 1 ET Contours.

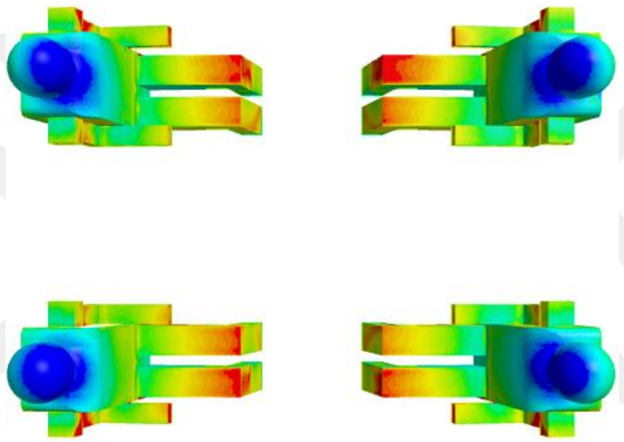

Figure 6.20 : Case 2 ET Contours.

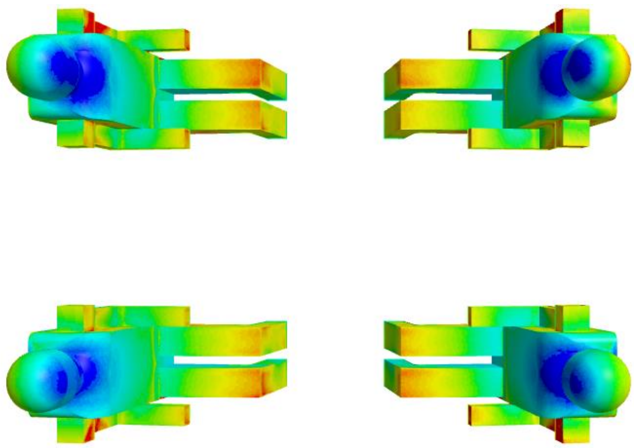

Figure 6.21 : Case 3 ET Contours.

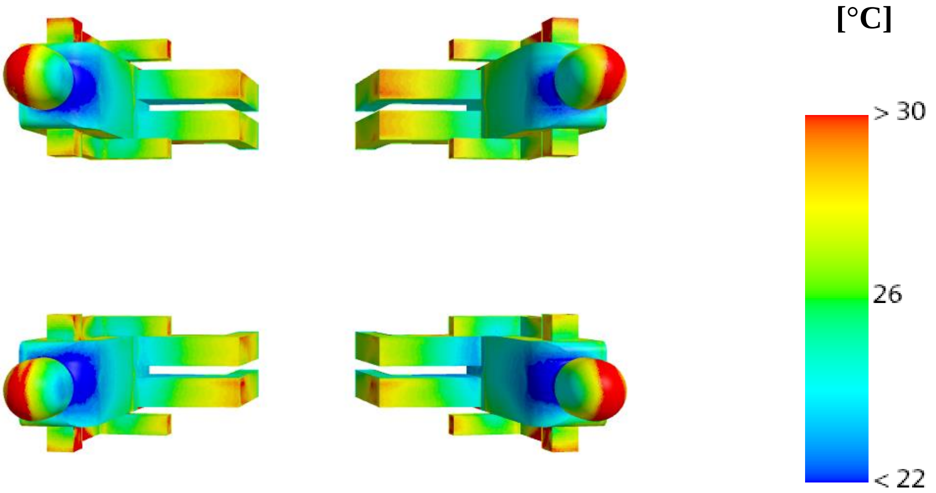

Figure 6.22 : Case 4 ET Contours.

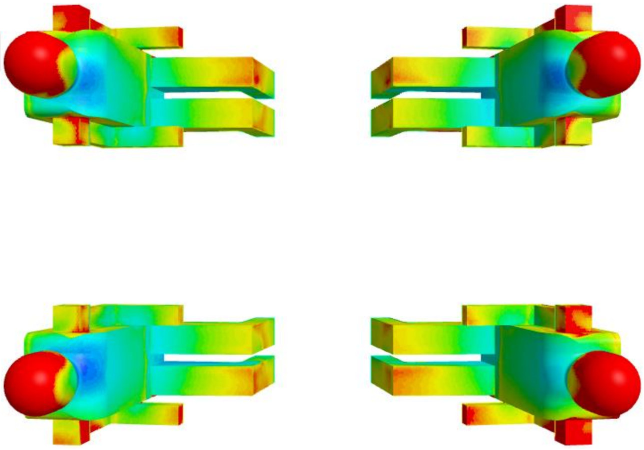

Figure 6.23 : Case 5 ET Contours.

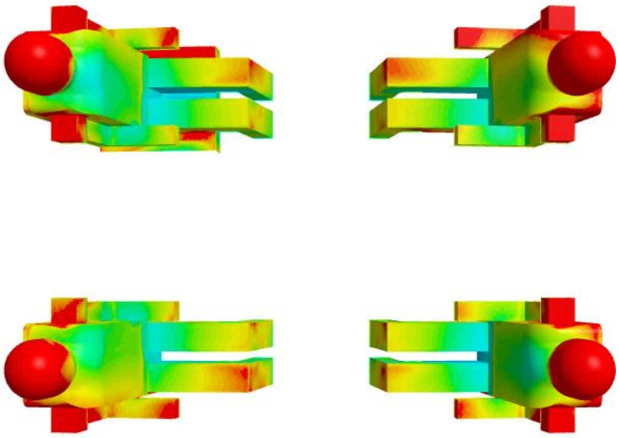

Figure 6.24 : Case 6 ET Contours.

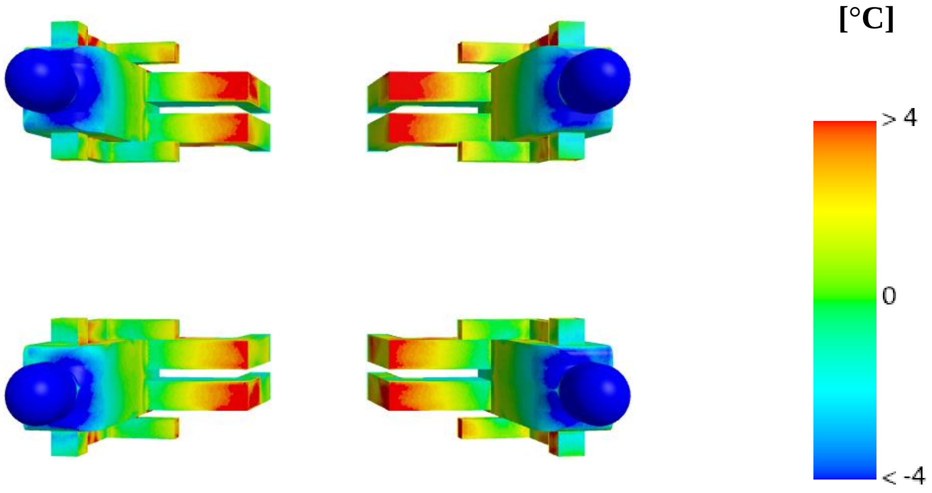

Figure 6.25 : Case 1 EDT Contours.

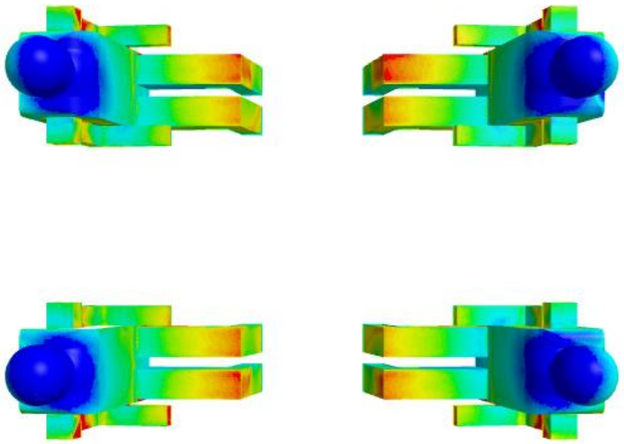

Figure 6.26 : Case 2 EDT Contours.

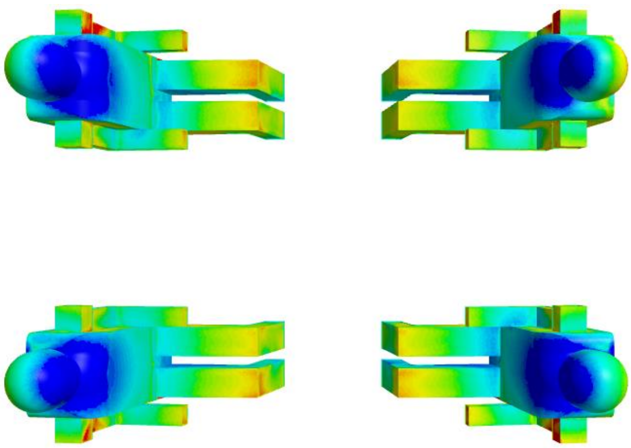

Figure 6.27 : Case 3 EDT Contours.

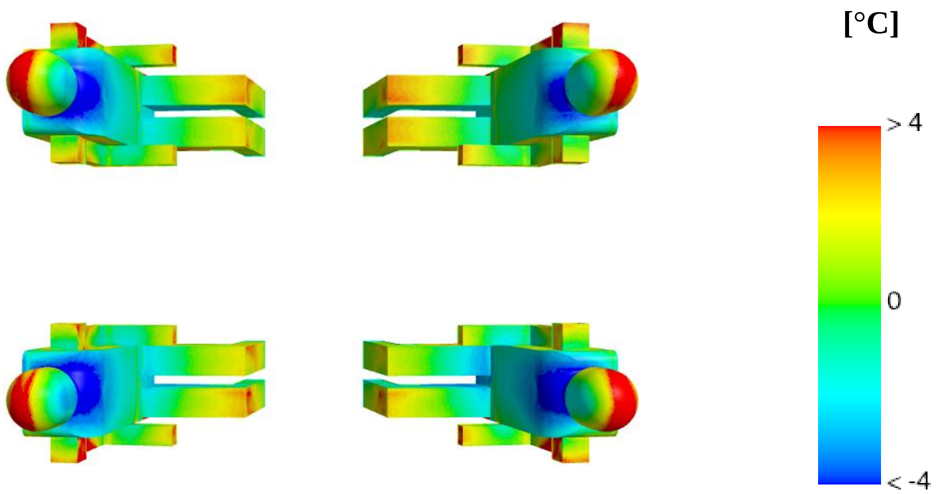

Figure 6.28 : Case 4 EDT Contours.

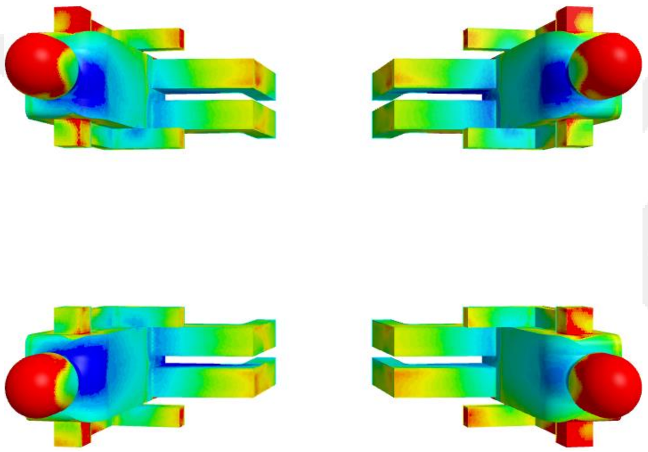

Figure 6.29 : Case 5 EDT Contours.

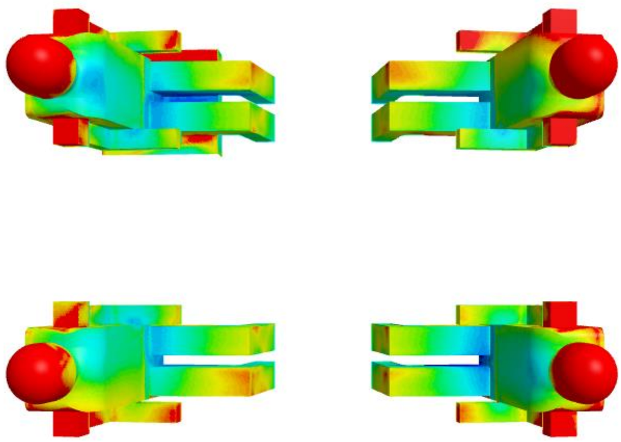

Figure 6.30 : Case 6 EDT Contours.

It is identified that the gasper positions in Case 3 and Case 4 are the most suitable for ensuring thermal comfort. In those analyses, the gasper is positioned symmetrically with respect to the passenger. To investigate the effects of asymmetrical gasper placement on thermal comfort, further analyses are conducted for Case 7 to Case 10. The details of the gasper positions are summarized in Table 6.7, while Figure 6.31 illustrates the relative positions and numbering of the gaspers with respect to the passenger.

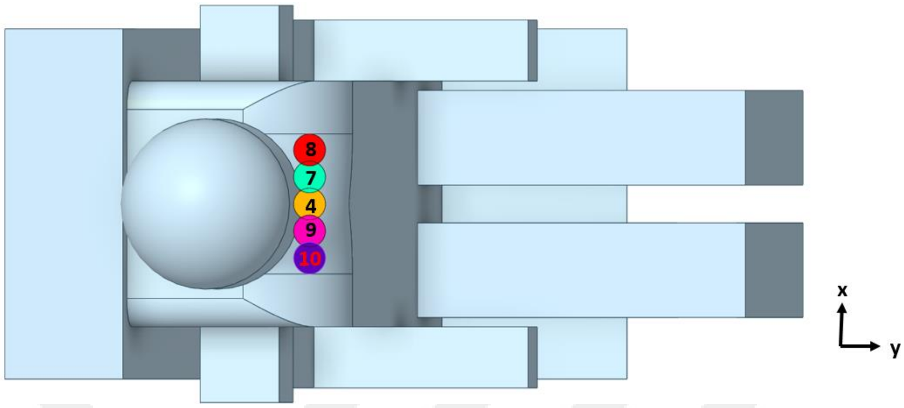

Figure 6.31 : Gasper Locations for Case 7-10.

Table 6.7 : Gasper Positions and Locations for Case 7-10.

CASES	GASPERS	Distance from Referance Gasper Location in x-direction (mm)	Distance from Referance Gasper Location in y-direction (mm)
Case 4	G4	0	0
Case 7	G7	30	0
Case 8	G8	60	0
Case 9	G9	-30	0
Case 10	G10	-60	0

The effects of gaspers placed at specific distances from the symmetry axis on thermal comfort will be examined based on the analysis results. Analyses are conducted for the gasper positions specified in Table 6.7, and the ET and EDT temperature results are examined for Passenger 1. Figure 6.32 and Figure 6.33 present the average temperature values by body segment.

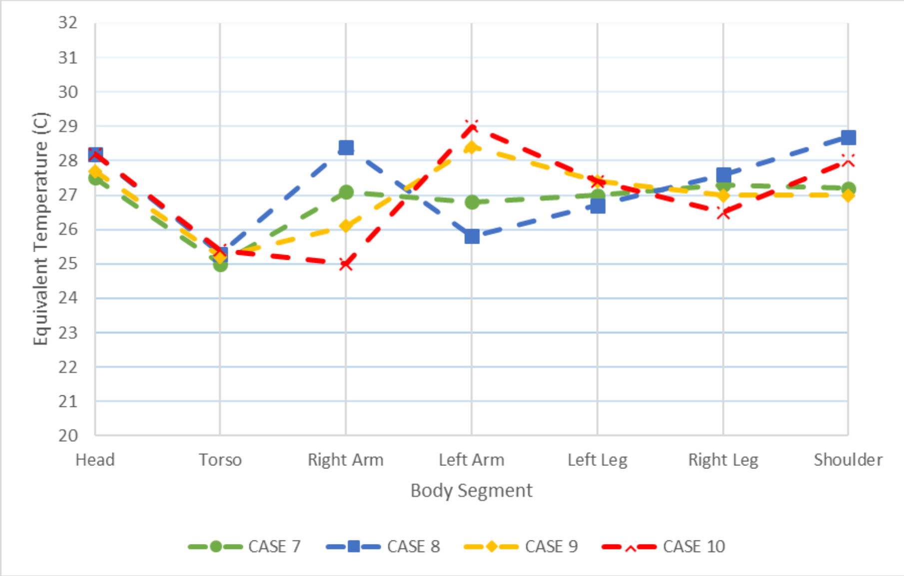

Figure 6.32 : Average ET Temperatures of Body Segement for Case 7-10.

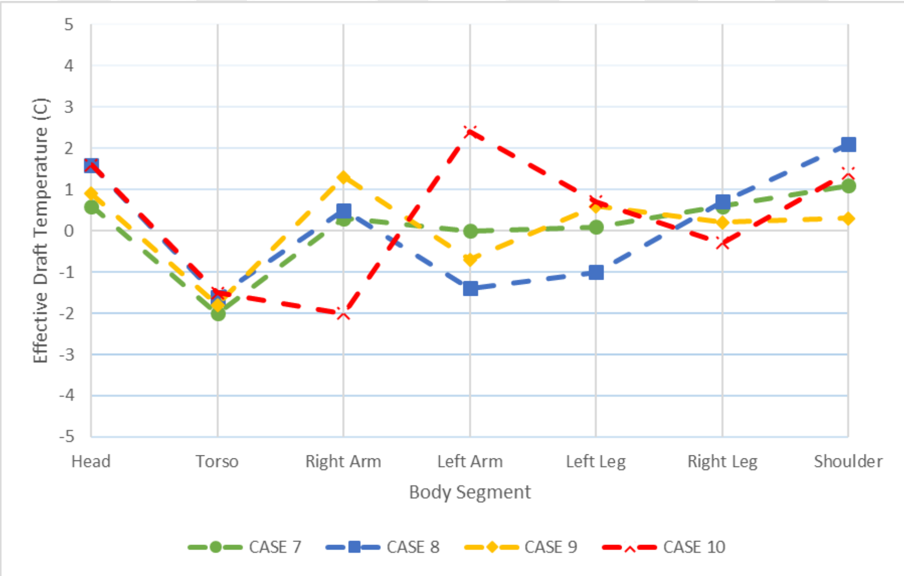

Figure 6.33 : Average EDT Temperatures of Body Segement for Case 7-10.

The gasper positions in Case 7 and Case 9 are offset by 30 mm from the reference location, whereas in Case 8 and Case 10, this offset is increased to 60 mm. Based on the analysis results, it is evident that the ET and EDT temperature values in Case 7 and Case 9 remain within acceptable thermal comfort limits. However, as the gasper moves further from the passenger's symmetry axis, noticeable asymmetries in temperature distribution emerge. For example, in Case 8, lower temperatures are recorded on the left side of Passenger 1, while the right side shows elevated temperatures compared to those in Case 4. The ET temperature contours for Case 7 through Case 10 are illustrated in Figure 6.34, Figure 6.35, Figure 6.36 and Figure 6.37, respectively.

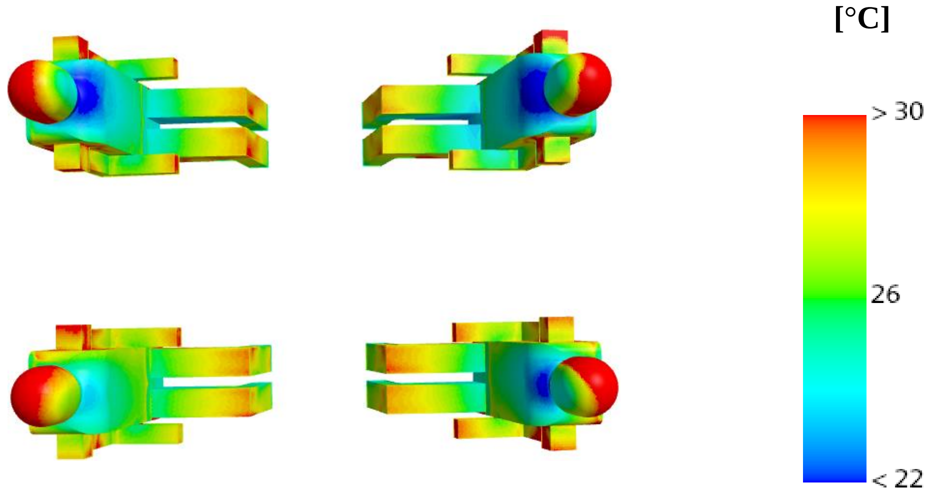

Figure 6.34 : Case 7 ET Contours.

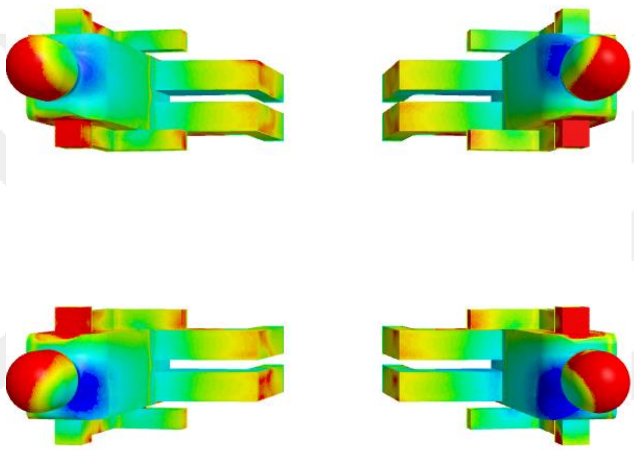

Figure 6.35 : Case 8 ET Contours.

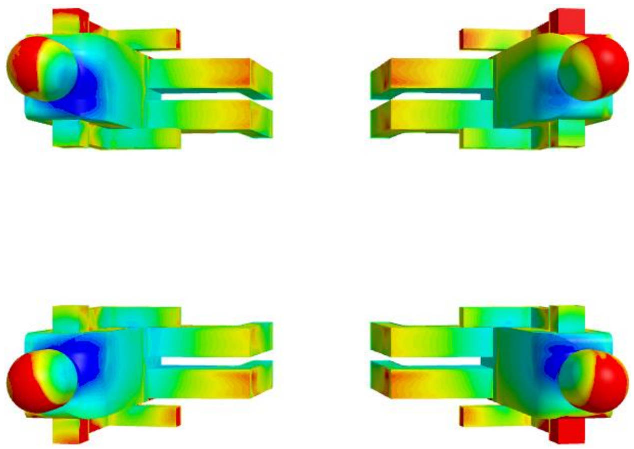

Figure 6.36 : Case 9 ET Contours.

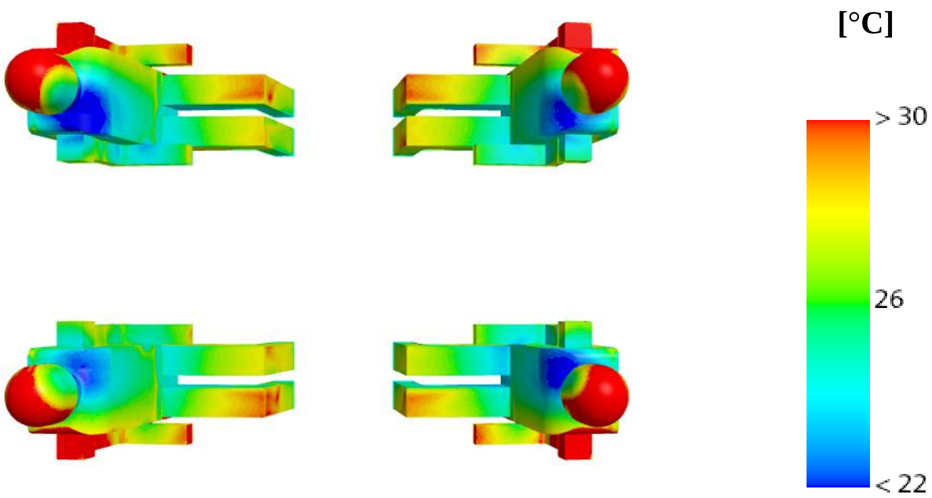

Figure 6.37 : Case 10 ET Contours.

The EDT temperature contours for Cases 7 through 10 are illustrated in Figure 6.38, Figure 6.39, Figure 6.40 and Figure 6.41, respectively.

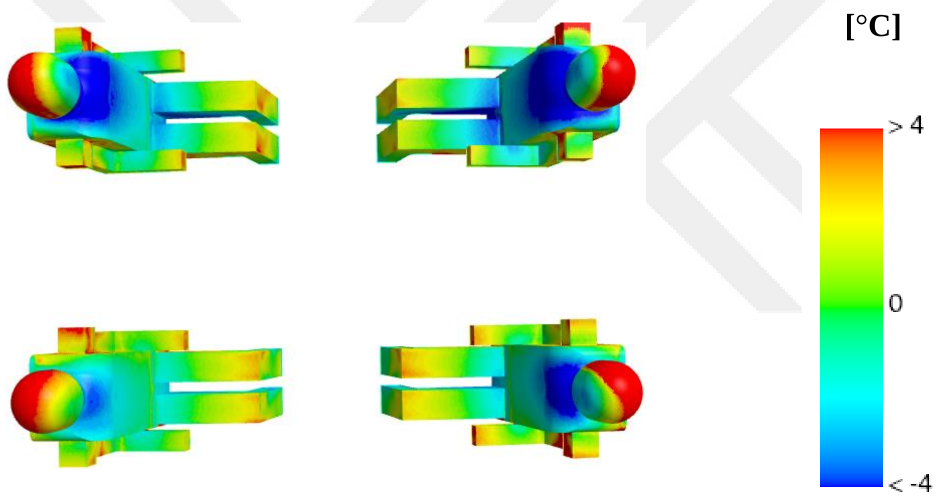

Figure 6.38 : Case 7 EDT Contours.

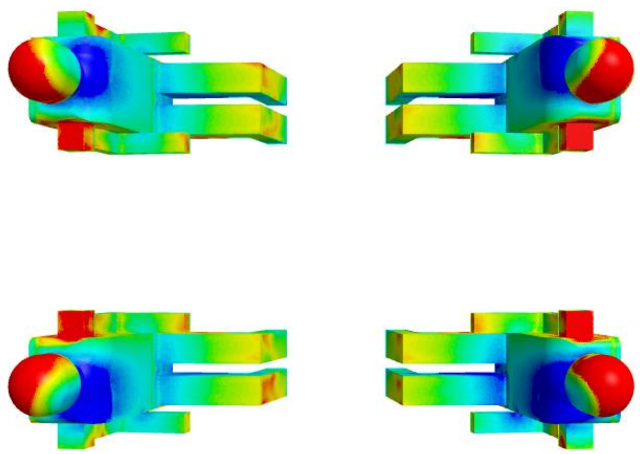

Figure 6.39 : Case 8 EDT Contours.

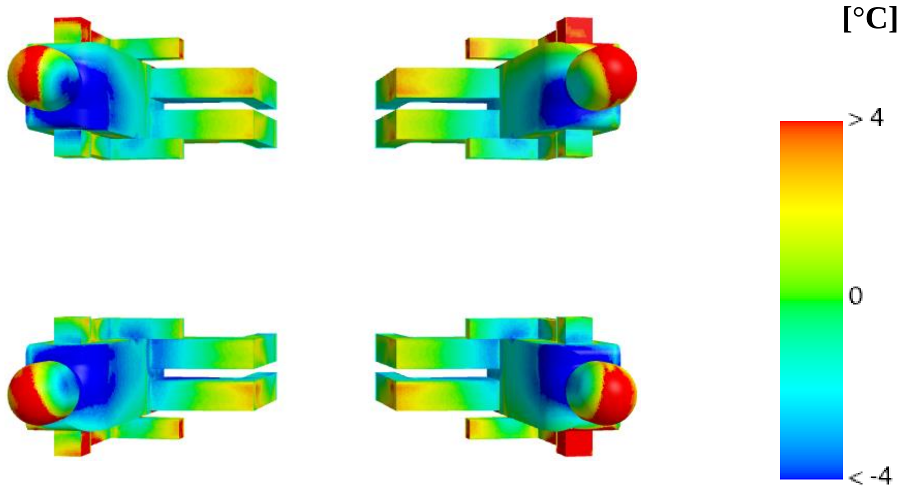

Figure 6.40 : Case 9 EDT Contours.

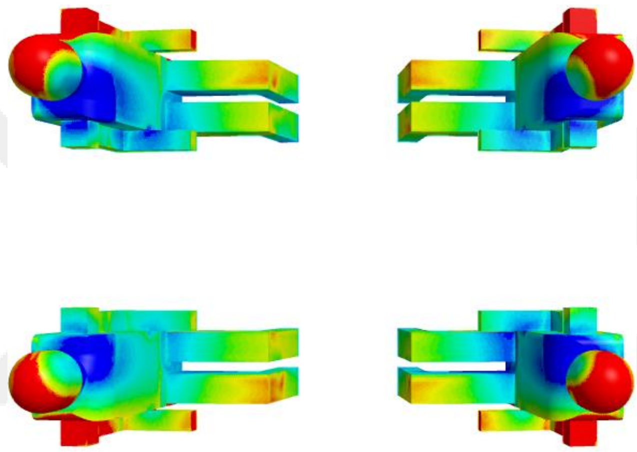

Figure 6.41 : Case 10 EDT Contours.

According to the analysis results, the position of the gasper plays a crucial role in ensuring the passenger's thermal comfort. The gasper should be positioned symmetrically with respect to the passenger's seating arrangement and 0-30 mm in front of the passenger's head level. If it is not feasible to position the gasper along the passenger's symmetry axis, placing it 30 mm to the side of the axis will not have a negative impact on thermal comfort.

6.5 Investigation of the Effect of Gasper & Main Outlet Flow Rate on Passenger Thermal Comfort

Based on the previously determined optimal gasper location, the influence of varying airflow rates at the gaspers and main outlets on thermal comfort was systematically analyzed. This investigation encompassed five distinct scenarios, representing conditions from fully open to fully closed gaspers, including several intermediate levels of openness. In all scenarios, the total airflow rate within the cabin was maintained constant. When the gaspers are partially or fully closed, the corresponding portion of the airflow was redistributed to the main outlets to ensure the overall airflow remained unchanged. In this analysis set, only the flow rate ratios of the gasper and main inlet were modified, while the other boundary conditions were kept as defined in Section 6.3.

Gaspers in aircraft cabins are typically adjustable by passengers, both in terms of airflow direction and flow rate. However, in this study, only the effect of different gasper airflow rates on thermal comfort was examined; variations in airflow direction are not considered. In each of the analyzed scenarios, gasper flow rates are simultaneously reduced, while flow rates from the main outlets are proportionally increased. Additionally, the airflow from both the gaspers and the main outlets is equally distributed among their respective outlets in the computational simulations. Details regarding the airflow rates and the analyzed scenarios are summarized in Table 6.8.

Table 6.8 : Gasper and Main Outlet Velocity for Case 11-14.

CASES	The Closure Ratio of the Gaspers	Gasper Outlet Velocity (m/s)	Main Outlet Velocity (m/s)
Case 4	0	10	1.5
Case 11	25	7,5	1,75
Case 12	50	5	2
Case 13	75	2,5	2,25
Case 14	100	0	2,5

For each scenario presented in Table 2, thermal comfort analyses are conducted, and the average ET and EDT values are obtained for Passenger 1. The objective of this investigation is to evaluate the role of personalized air outlets which are gaspers, in maintaining thermal comfort for each passenger. For the investigation of thermal comfort under varying gasper airflow rates, Case 4 gasper position is taken as the reference, and all analyses are conducted based on Gasper 4 location. Figure 6.42 and Figure 6.43 present the average ET and EDT values by body segment.

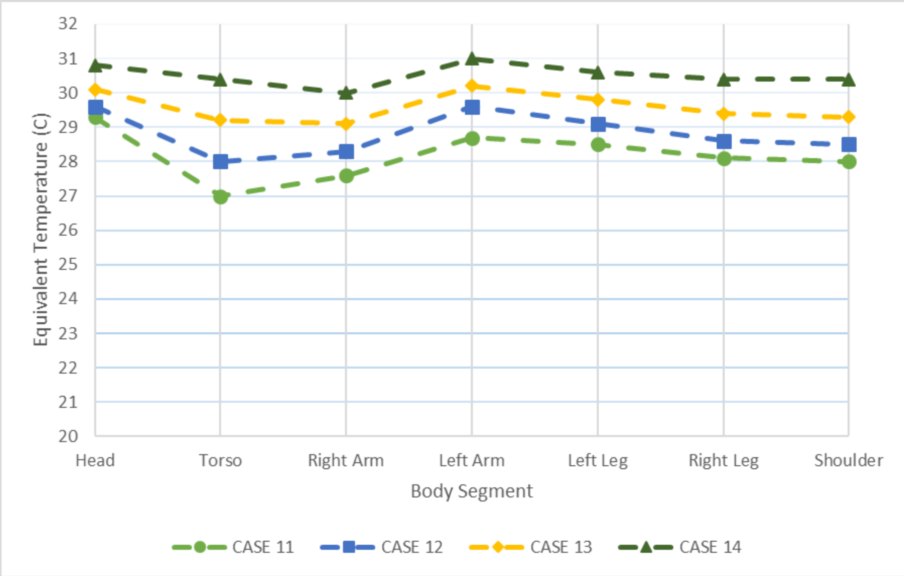

Figure 6.42 : Average ET Temperatures of Body Segement for Case 11-14.

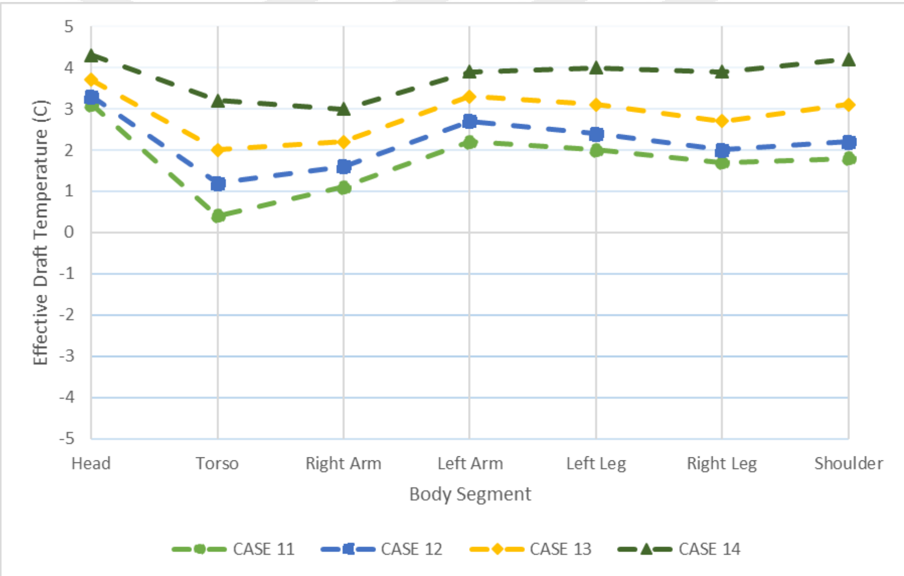

Figure 6.43 : Average EDT Temperatures of Body Segement for Case 11-14.

According to the analysis results, as the personalized airflow supplied to the passengers decreases, thermal comfort is gradually affected in a negative way. Although the airflow provided through the gaspers is also supplied from the main outlets, it has no direct effect on the passengers and primarily helps to reduce the overall cabin temperature. It is observed that gasper air outlets are not only effective for the thermal comfort of the head and chest regions, but also directly influence the comfort of the entire body. This highlights the importance of localized ventilation systems in maintaining optimal thermal conditions for each passenger. Ensuring adequate airflow through gaspers can significantly enhance the perceived comfort, especially during high external temperature conditions. Additionally, uniform airflow distribution across all seating positions is critical for achieving consistent comfort levels throughout the cabin. The ET temperature contours for the passengers in Cases 11 to 14 are presented in Figure 6.44, Figure 6.45, Figure 6.46 and Figure 6.47 respectively.

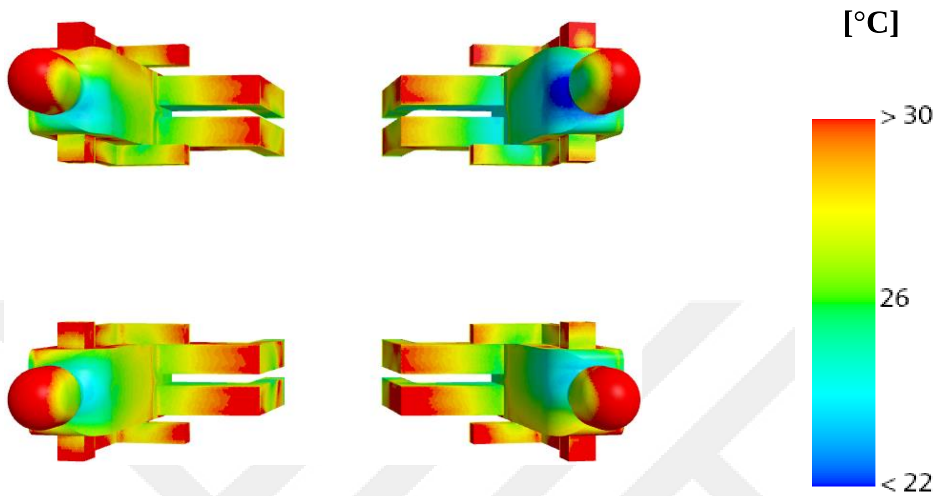

Figure 6.44 : Case 11 ET Contours.

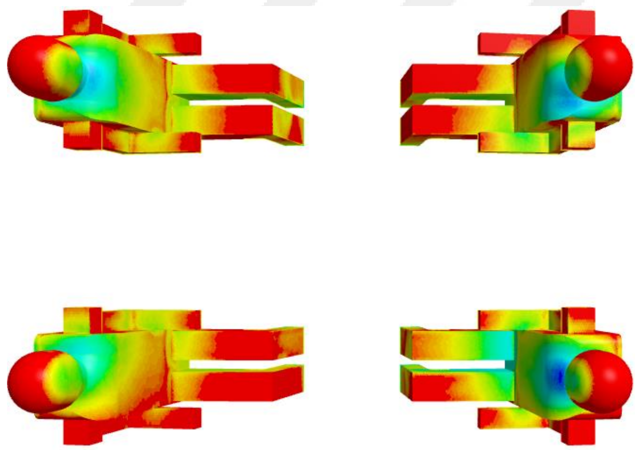

Figure 6.45 : Case 12 ET Contours.

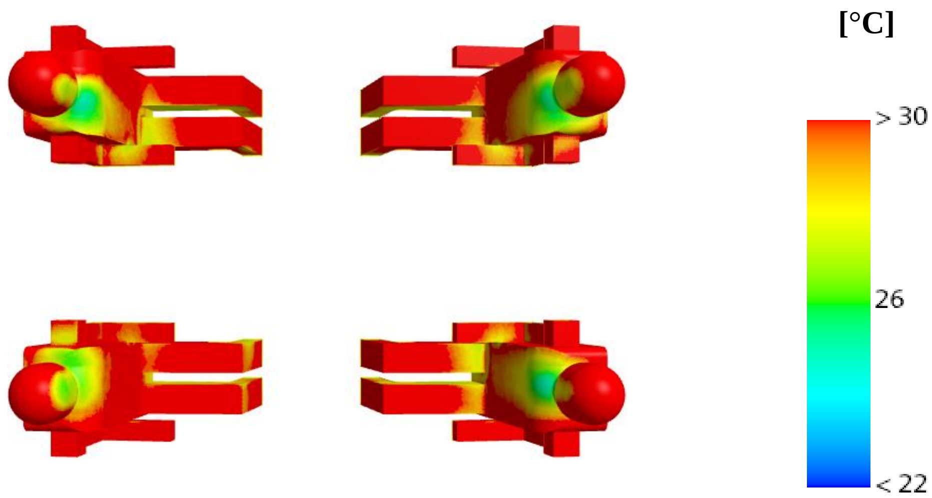

Figure 6.46 : Case 13 ET Contours.

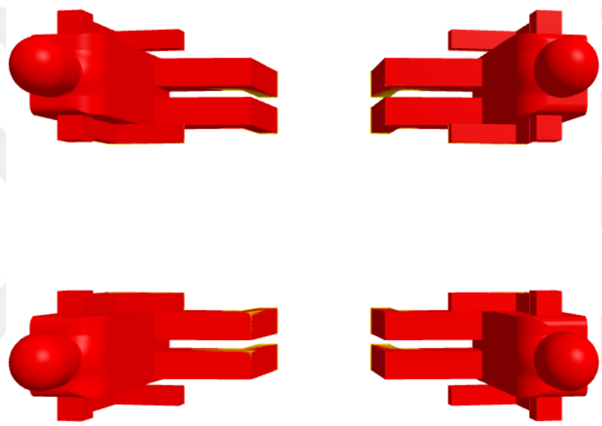

Figure 6.47 : Case 14 ET Contours.

In this analysis set, which investigates the effect of the airflow rate supplied by the gasper on thermal comfort, it is observed that a reduction in the gasper airflow leads to passenger discomfort and a failure to maintain adequate thermal comfort. When examining the results based on ET temperatures, it is seen that a decrease in airflow rate from the gasper primarily affects thermal comfort in the leg region. The airflow provided by the main outlets does not directly lower the ET temperatures of the passengers but rather contributes to reducing the overall cabin temperature. It is observed that a decrease in gasper airflow leads to a deterioration of thermal comfort across all regions of the body. Results indicate that a reduction in gasper airflow rates compromises the thermal comfort of passengers. Therefore, it is necessary to also evaluate the results using EDT temperature values.Figure 6.48, Figure 6.49, Figure 6.50, Figure 6.51 present the EDT temperature distributions over the passenger bodies. These contours reveal that thermal discomfort becomes more pronounced, especially in areas distant from the gasper airflow. This emphasizes the importance of sufficient and well-directed airflow from the gasper to maintain consistent thermal comfort throughout the body.

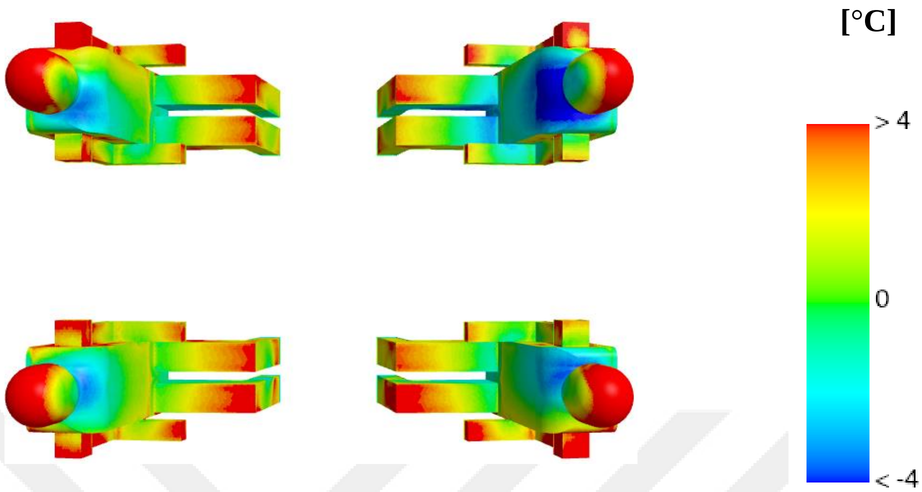

Figure 6.48 : Case 11 EDT Contours.

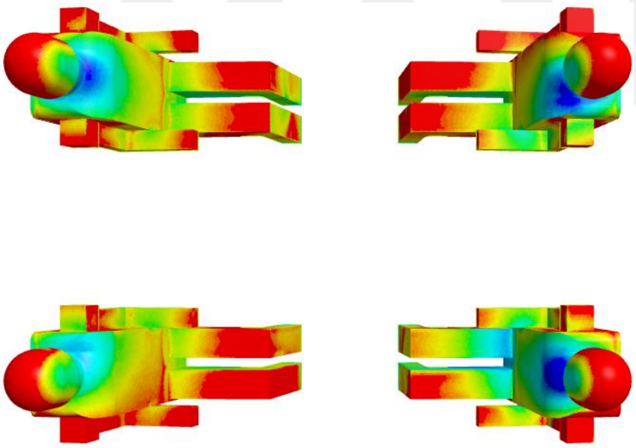

Figure 6.49 : Case 12 EDT Contours.

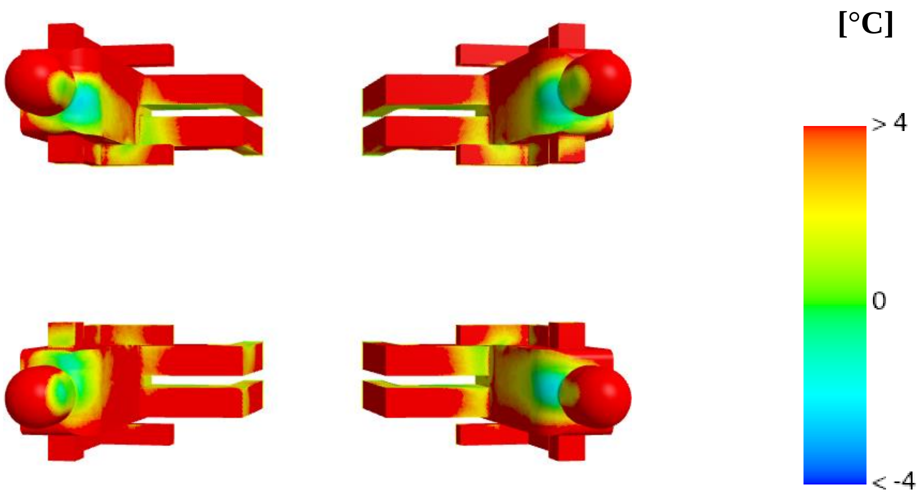

Figure 6.50 : Case 13 EDT Contours.

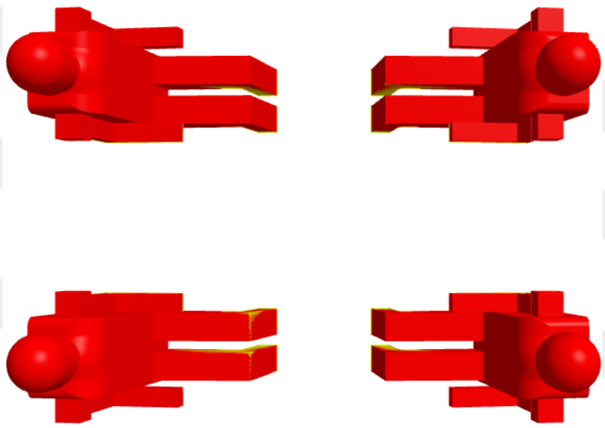

Figure 6.51 : Case 14 EDT Contours.

An examination of the EDT temperature distributions over the passenger bodies reveals a consistent trend with the ET temperature results, indicating a decline in thermal comfort as the gasper airflow rate decreases. The overall findings of the analysis underscore the critical importance of personalized air outlets, such as gaspers, in maintaining acceptable levels of thermal comfort within the cabin environment.

6.6 Investigation of the Effect of Gasper Cross-Sectional Area Change on Passenger Thermal Comfort

According to the principle of mass conservation, in flows where the density is assumed to be constant, an increase in cross-sectional area results in a decrease in velocity. The case where the gasper outlet velocity increases as the gasper cross-sectional area decreases is consistent with this principle. However, according to ISO 7730 standards, both an increase and a decrease in the airflow velocity delivered to passengers may negatively affect thermal comfort. In this section, the effect of varying the gasper cross-sectional area on thermal comfort is investigated. During the analysis, it is assumed that the airflow rates supplied through both the gaspers and the main air outlets remain unchanged. The positions of the gaspers and main air outlets remain unchanged throughout the analysis of this parameter. The gaspers are positioned according to the locations defined in Section 6.3, and the analyses are carried out accordingly. Table 6.9 presents the variations in gasper cross-sectional areas and the corresponding gasper outlet velocities for each case.

Table 6.9 : Gasper Cross Section Area and Velocity for Case 15-18.

CASES	Gasper Cross-Section Area	Gasper Outlet Velocity (m/s)
Case 4	A	10
Case 15	0.75 A	13.33
Case 16	0.5 A	20
Case 17	1.25 A	8
Case 18	1.5 A	6.66

In this analysis set, only the gasper cross-sectional area is modified to investigate its effect on thermal comfort. The other boundary conditions remained the same as those specified in Section 6.3. The regional averages of ET and EDT temperatures are shown in Figure 6.52 and Figure 6.53, respectively.

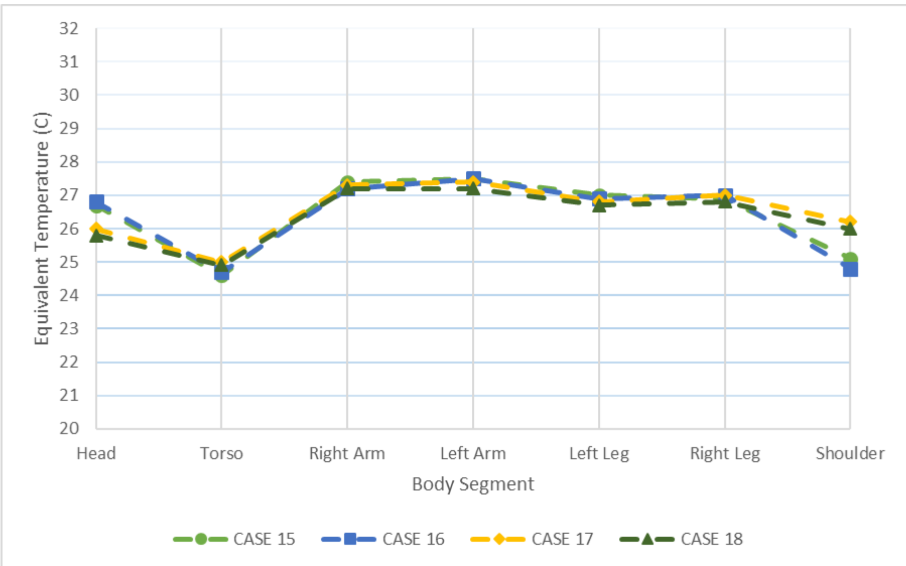

Figure 6.52 : Average ET Temperatures of Body Segement for Case 15-18.

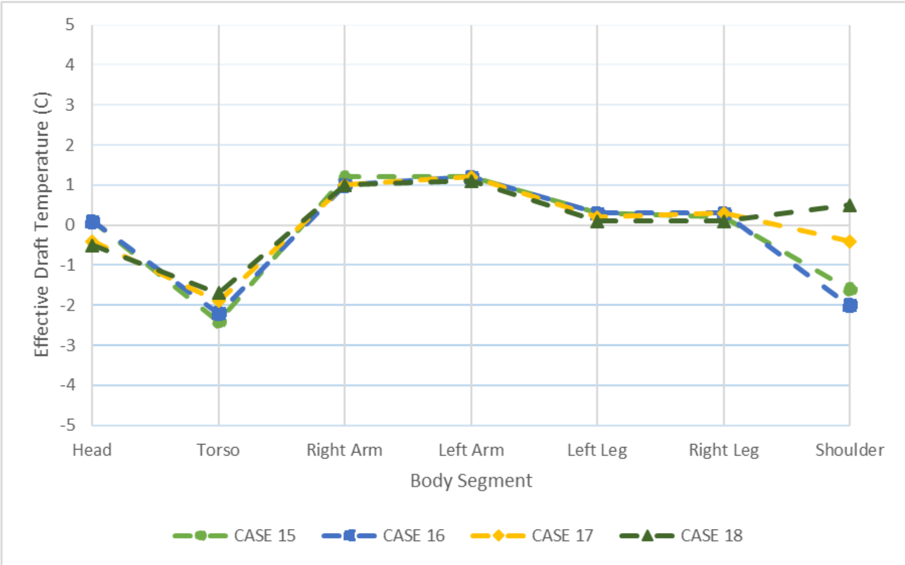

Figure 6.53 : Average EDT Temperatures of Body Segement for Case 15-18.

It is observed that a decrease in the cross-sectional area has an effect on the ET and EDT temperatures in the shoulder and head regions. For other areas of the body, it is seen that they are more influenced by the ambient air temperature rather than the gasper air exit velocity, and have a greater impact on thermal comfort. For a clearer assessment of the effect of cross-sectional area, ET contour plots are presented in Figure 6.54, Figure 6.55, Figure 6.56, Figure 6.57, while EDT contour plots are shown in Figure 6.58, Figure 6.59, Figure 6.60, Figure 6.61.

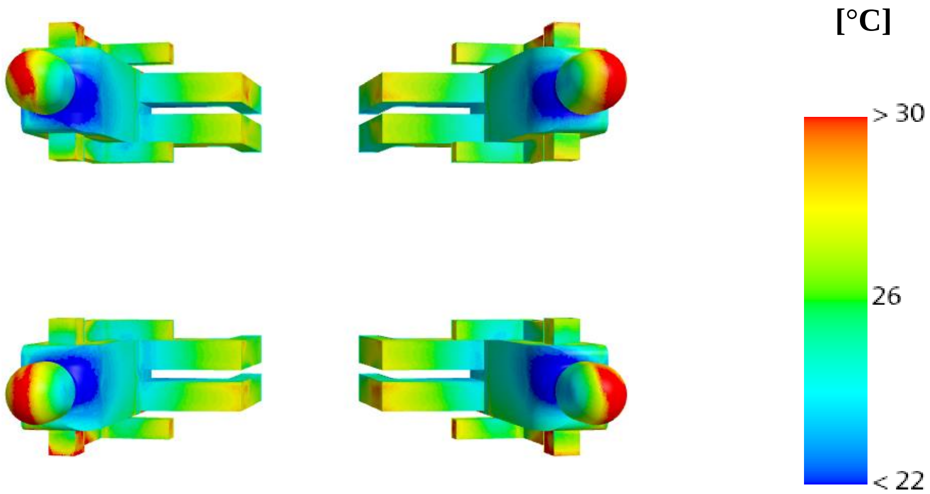

Figure 6.54 : Case 15 ET Contours.

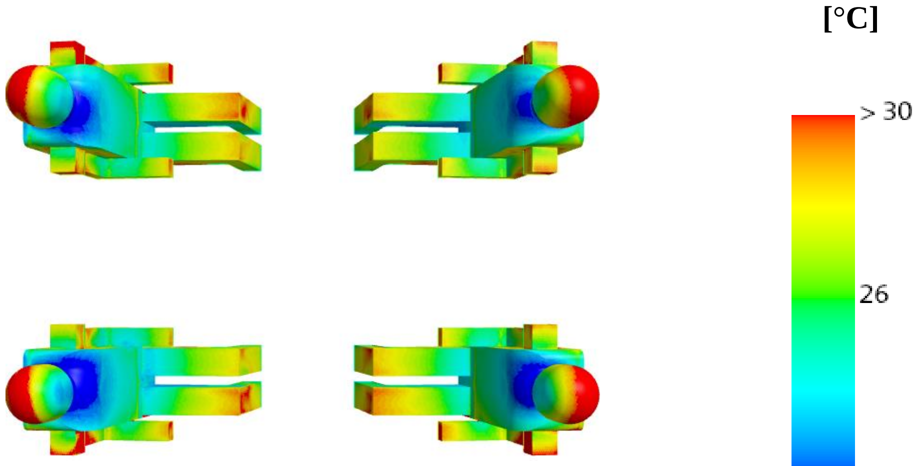

Figure 6.55 : Case 16 ET Contours.

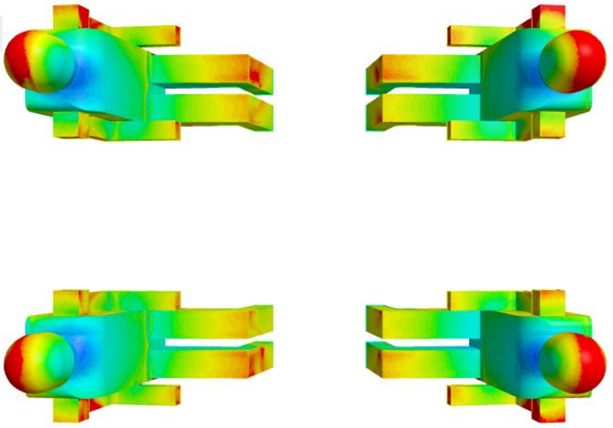

Figure 6.56 : Case 17 ET Contours.

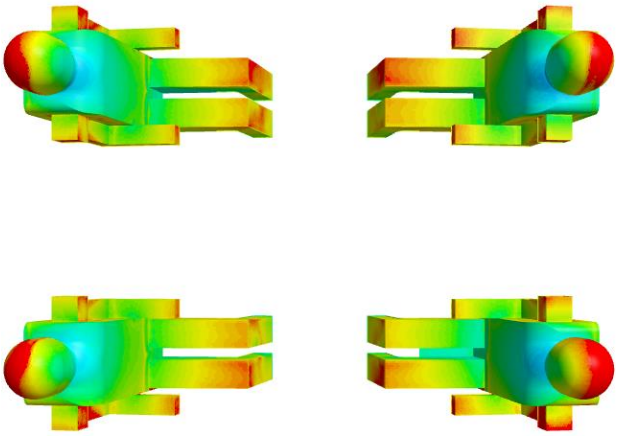

Figure 6.57 : Case 18 ET Contours.

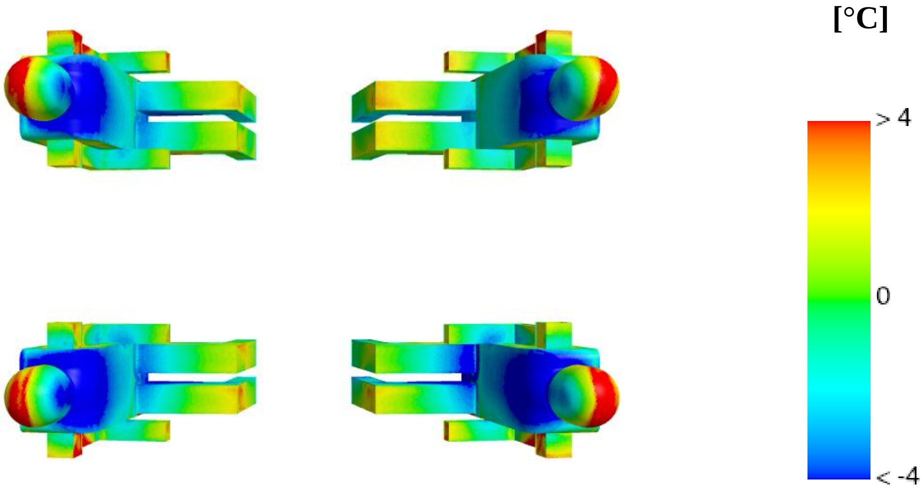

Figure 6.58 : Case 15 EDT Contours.

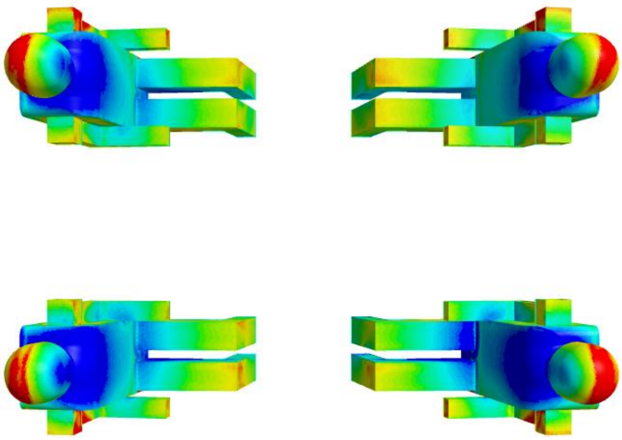

Figure 6.59 : Case 16 EDT Contours.

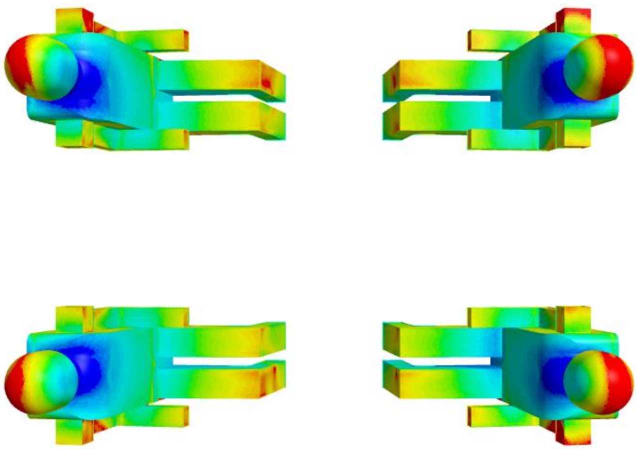

Figure 6.60 : Case 17 EDT Contours.

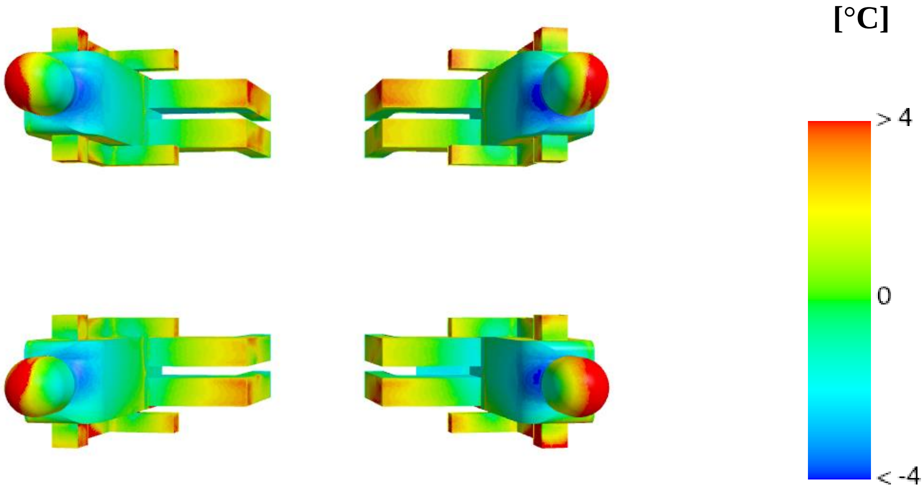

Figure 6.61 : Case 18 EDT Contours.

With the decrease in gasper cross-sectional area and the resulting increase in air velocity, passengers tend to feel cold in the shoulder region, negatively affecting thermal comfort. Conversely, when the gasper cross-sectional area increases and the velocity decreases, a warm sensation is experienced in the head and shoulder regions, which can also adversely impact thermal comfort.

6.7 Investigation of the Relationship Between Supplied Cold Air Temperature & Outside Air Temperature

In this section, the relationship between the supplied cabin air temperature and the outside ambient air temperature is investigated. In the previous sections, the ambient air temperature was assumed to be 50°C, which is consistent with the upper thermal envelope of current-generation helicopters. In those analyses, thermal comfort for passengers was achieved by supplying cold air into the cabin when the outside air temperature was 50°C. In this section, the ambient air temperature is considered as a variable, and adjustments are made to the supply air temperature accordingly to maintain passenger thermal comfort. The other parameters, boundary conditions, and assumptions are the same as those presented in Section 6.3. In this analysis set, the air temperatures supplied to the environment to ensure passenger thermal comfort are determined for external ambient temperatures of 50°C, 48°C, 46°C, 44°C, 42°C, and 40°C. While examining the analysis set, for an ambient temperature of 50 °C, the supplied air temperature is fixed at 8 °C. The analysis investigates whether passenger comfort is maintained despite variations in ambient temperature. While determining the required air supply temperatures for the given ambient conditions, the case of supplying 8 °C air to the cabin was also considered. Although an 8 °C supply air temperature was defined for an ambient temperature of 50 °C, maintaining the same supply air temperature at lower ambient temperatures may negatively affect passenger thermal comfort. Table 6.10 presents the scenarios and the corresponding supply air temperatures.

Table 6.10 : Outside Air & Supplied Air Temperatures by Cases

Cases	Outside Air Temperature (°C)	Supplied Air Temperature (°C)
Case 19	48	8
Case 20	48	8.4
Case 21	46	8
Case 22	46	9.6
Case 23	44	8
Case 24	44	11.9
Case 25	42	8
Case 26	42	13.5
Case 27	40	8
Case 28	40	14.8

An iterative solution method is employed to determine the appropriate supply air temperature based on the outside air temperature. Initially, air at 8°C is supplied to the cabin regardless of the ambient temperature, and the thermal comfort of the passengers was observed. The aim of the study in this section is to identify the cold air supply that ensures passenger thermal comfort under different environmental conditions. Currently, iterative analysis studies to maintain such thermal comfort are not conducted in modern aircraft. Therefore, in this thesis, adjusting the cabin air temperature according to the outside ambient temperature to provide passenger thermal comfort represents a novel approach. In cases where comfort could not be achieved or decreased, iterative adjustments are made to the supply air temperature, and the most suitable temperatures are presented in Table 6.10. The ET temperature contours on the passengers are shown in Figure 6.63, Figure 6.64, Figure 6.65, Figure 6.66, Figure 6.67, Figure 6.68, Figure 6.69, Figure 6.70 and Figure 6.71.

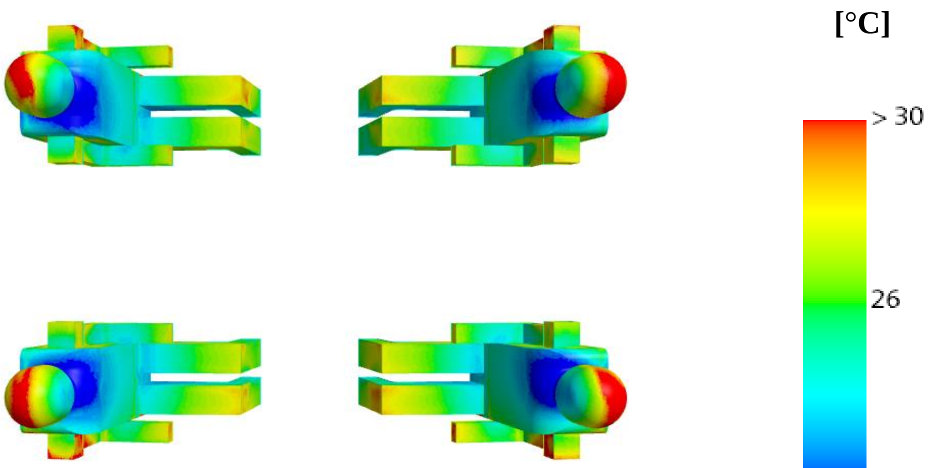

Figure 6.62 : Case 19 ET Contours.

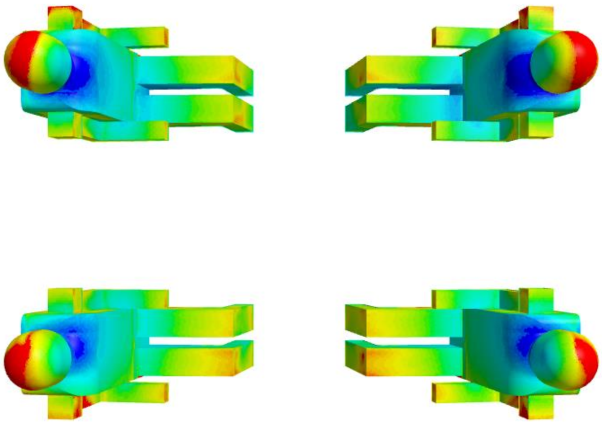

Figure 6.63 : Case 20 ET Contours.

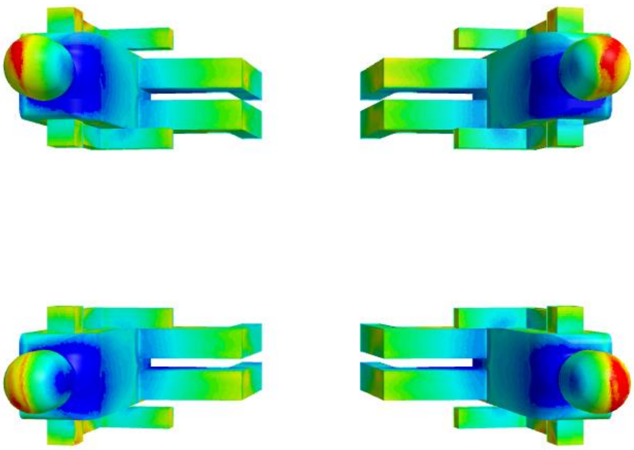

Figure 6.64 : Case 21 ET Contours.

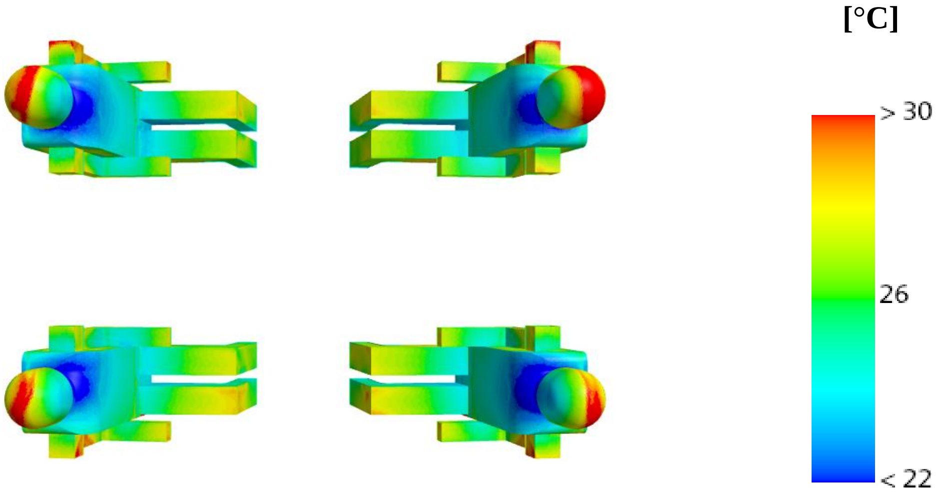

Figure 6.65 : Case 22 ET Contours.

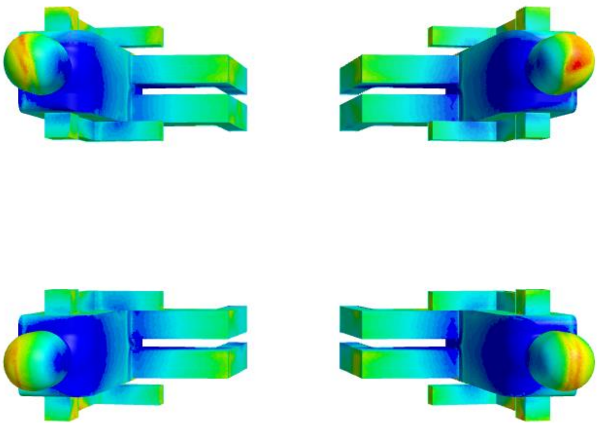

Figure 6.66 : Case 23 ET Contours.

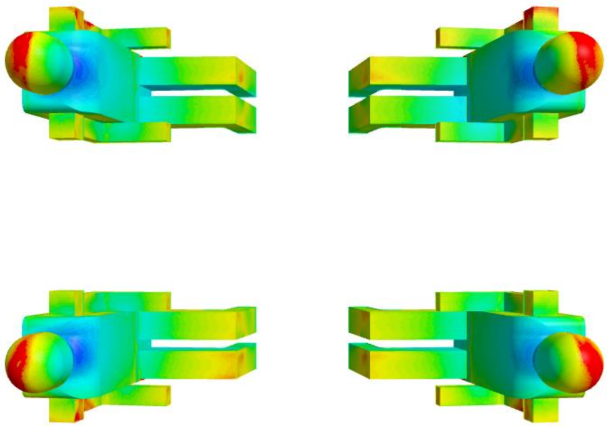

Figure 6.67 : Case 24 ET Contours.

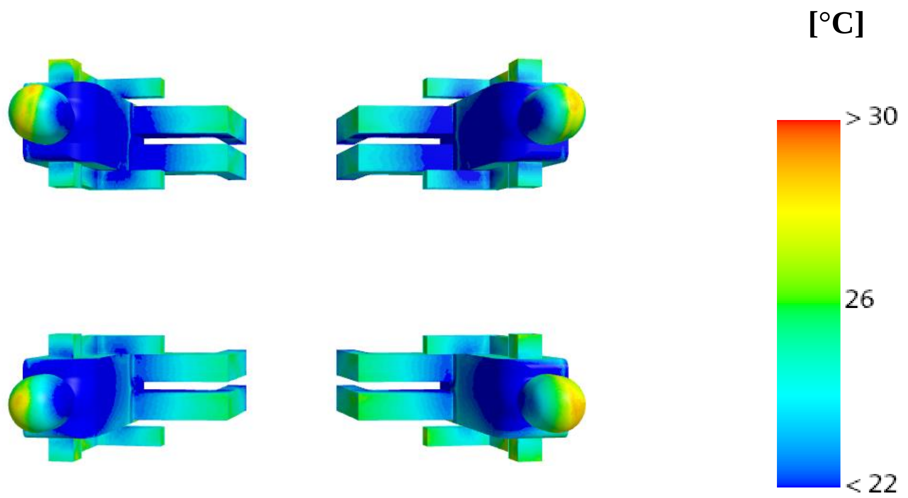

Figure 6.68 : Case 25 ET Contours.

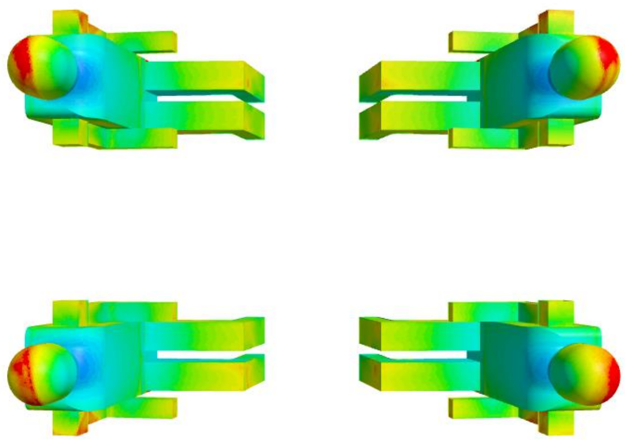

Figure 6.69 : Case 26 ET Contours.

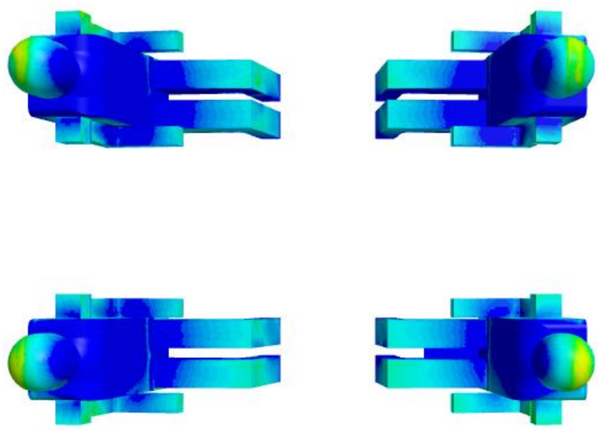

Figure 6.70 : Case 27 ET Contours.

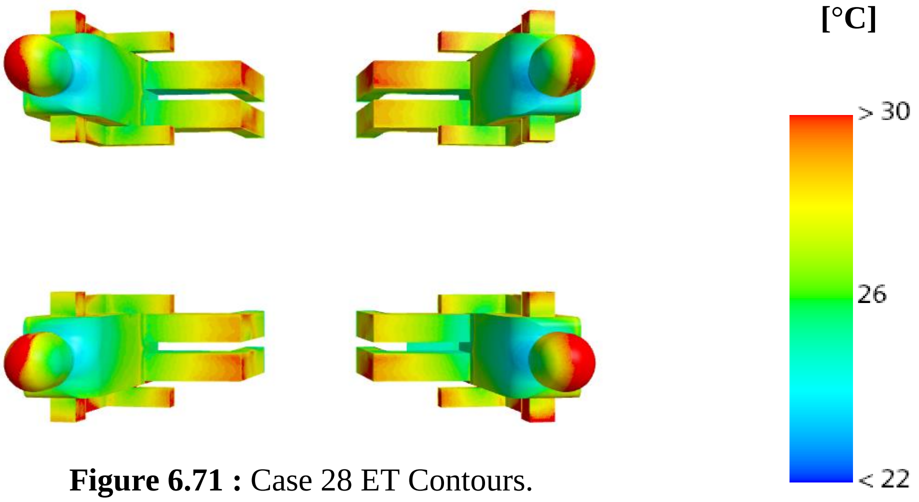

Figure 6.71 : Case 28 ET Contours.

The EDT temperature contours on the passengers are shown in Figure 6.72, Figure 6.73, Figure 6.74, Figure 6.75, Figure 6.76, Figure 6.77, Figure 6.78, Figure 6.79, Figure 6.80 and Figure 6.81

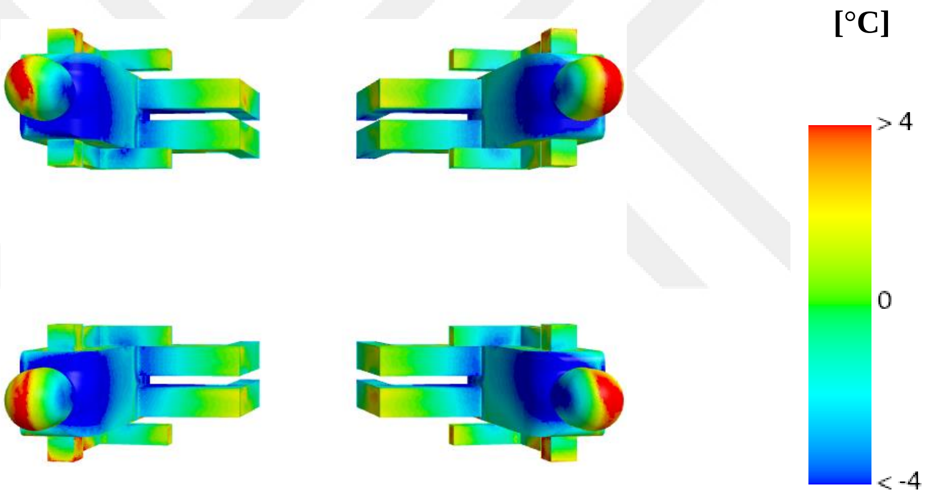

Figure 6.72 : Case 19 EDT Contours.

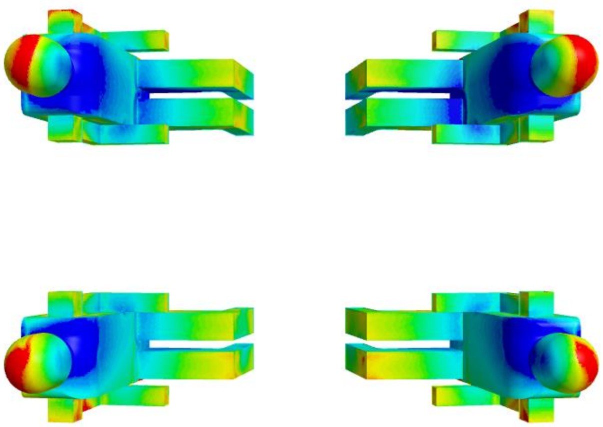

Figure 6.73 : Case 20 EDT Contours.

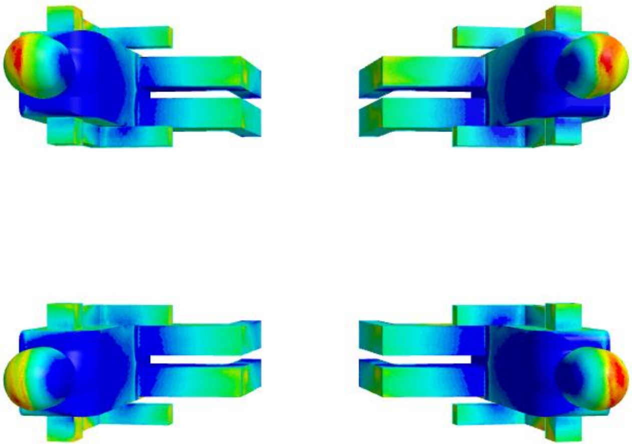

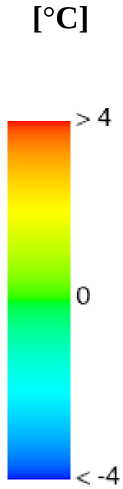

Figure 6.74 : Case 21 EDT Contours.

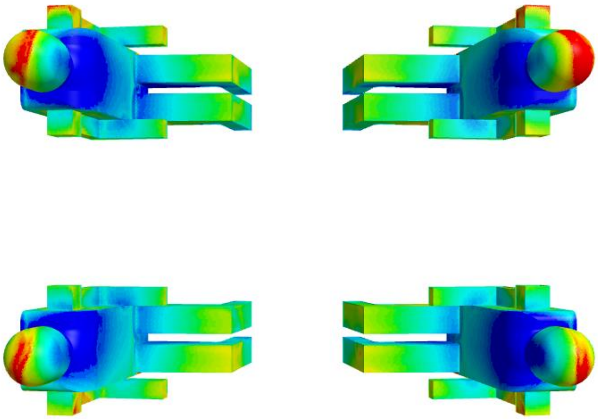

Figure 6.75 : Case 22 EDT Contours.

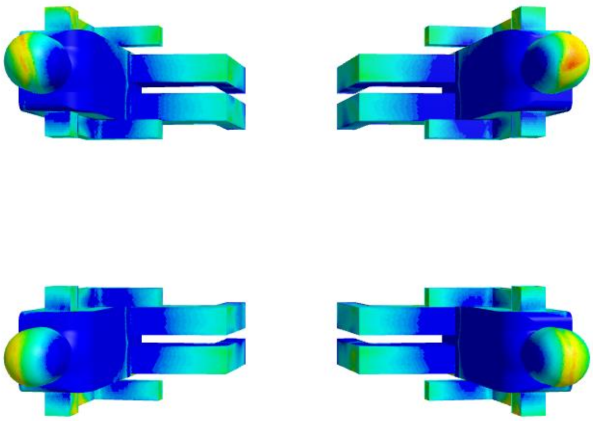

Figure 6.76 : Case 23 EDT Contours.

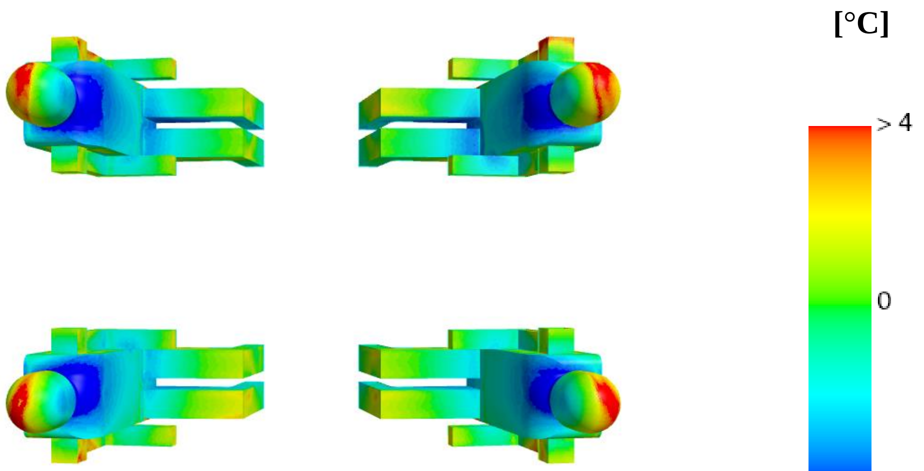

Figure 6.77 : Case 24 EDT Contours.

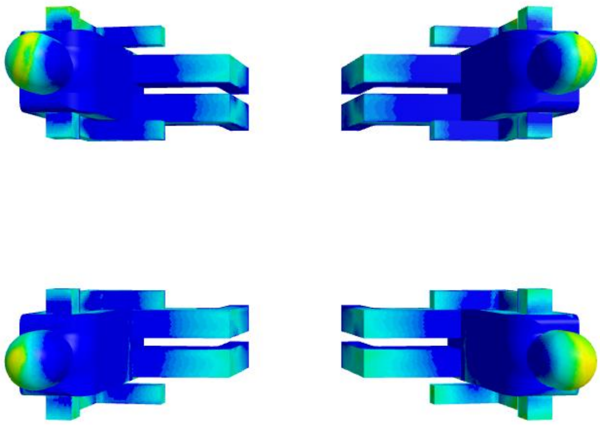

Figure 6.78 : Case 25 EDT Contours.

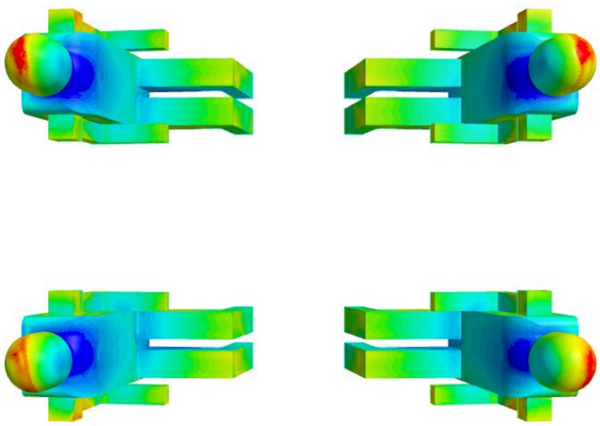

Figure 6.79 : Case 26 EDT Contours.

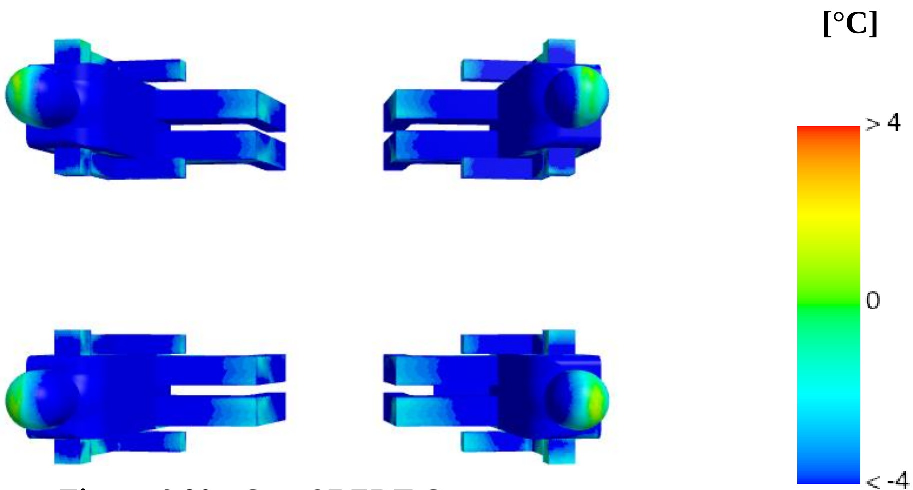

Figure 6.80 : Case 27 EDT Contours.

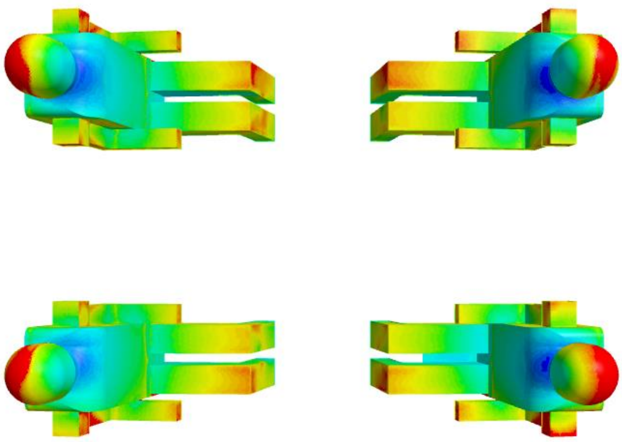

Figure 6.81 : Case 28 EDT Contours.

When the analysis results are evaluated, it is observed that as the outside air temperature decreases and the supplied cabin air temperature remains constant, passengers begin to feel cold, and thermal comfort cannot be achieved. It has been determined that thermal comfort is ensured when the temperature of the air supplied to the helicopter cabin is adjusted according to the external ambient temperature.

In addition to this section, according to the SAE ARP292 (2003) recommendation, an air velocity between 1–3 m/s around the passenger's head is suggested to ensure thermal comfort. Based on Case 28, the velocity contours on the passenger are shown in Figure 6.82 and Figure 6.83.

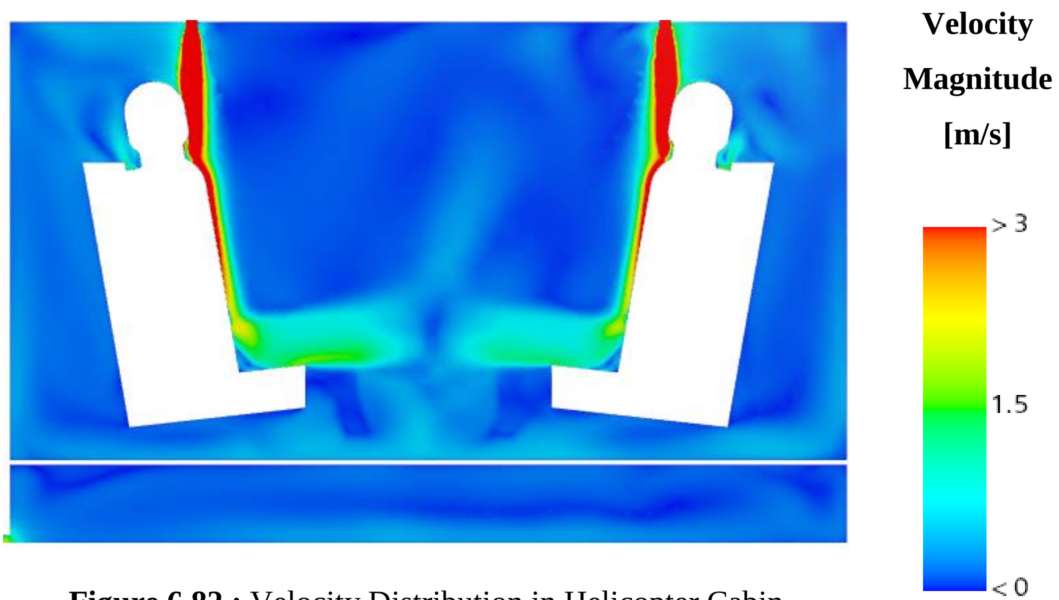

Figure 6.82 : Velocity Distribution in Helicopter Cabin.

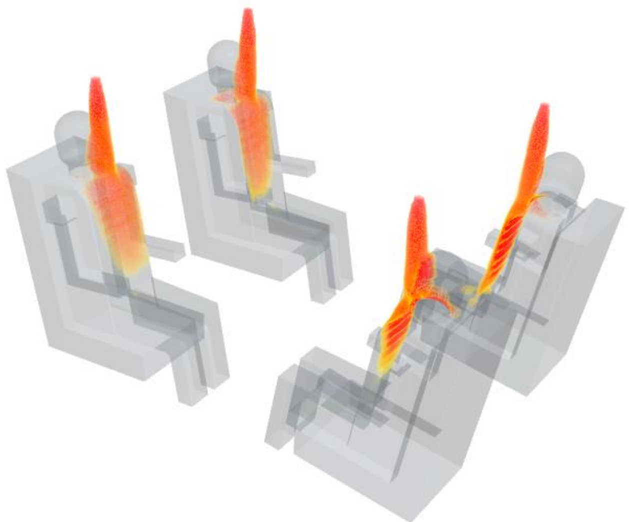

Figure 6.83 : Velocity Distribution on Passangers.

Upon examining the velocity contours, it is observed that the air velocity at the passenger's head level remains below 3 m/s, with an average velocity of approximately 1 m/s. This indicates that the gasper position and the overall design comply with the relevant standards.

7. CONCLUSIONS AND RECOMMENDATIONS

In this study, the parameters affecting the thermal comfort of passengers inside a helicopter cabin are investigated. The work begins with a literature review of existing research on aircraft and thermal comfort. The study is conducted numerically using the commercial CFD software Star-CCM+. In order to validate the numerical model, a mesh and simulation study is performed based on an experimental study found in the literature.

To be used in the numerical analyses, cabin geometries representative of existing helicopters are modeled, and realistic human and seat models were developed in proportion to actual dimensions. Subsequently, parameters that influence passenger thermal comfort are identified and analyzed.

The findings obtained from this thesis study can be summarized as follows:

- Due to the air distribution and geometry within the helicopter cabin, non-uniform distributions of air velocity and air temperature are observed.
- In non-uniform environments such as helicopter cabins, the PMV and PPD indices proposed by Fanger (1970) are not valid indicators of thermal comfort. Analysis results show that temperature and air velocity values on passengers vary significantly from one body region to another. Since the Fanger method treats the human body as a single uniform entity, this approach is not suitable for such conditions.
- The ET thermal comfort parameter approach proposed by Madsen et al. (1978) and the EDT parameter approach introduced by Rydberg et al. (1949) can be used to assess thermal comfort in non-uniform environments such as helicopter cabins.
- In non-uniform environments, the thermal comfort of passengers shall be assessed by examining individual body regions separately, as air velocity and air temperature can vary significantly across different areas of the body. Using

average ET and EDT values for the entire body would be a coarse and less accurate approach.

- Personalized air outlets for passengers are crucial in ensuring thermal comfort. Even when the total airflow rate into the cabin remains constant, a reduction in gasper airflow significantly diminishes thermal comfort.
- The position of the gasper is one of the critical parameters in ensuring passenger thermal comfort. It has been observed that placing the gasper at a distance of 0–30 mm from the passenger's head level, aligned symmetrically with the passenger, provides optimal comfort. Additionally, when the gasper is positioned 0–30 mm to the left or right of the passenger's symmetry axis, thermal comfort can still be maintained. In other configurations, passengers may experience discomfort in terms of thermal comfort.
- It has been observed that when the gasper airflow rate remains constant, reducing the gasper cross-sectional area causes localized discomfort for passengers. Similarly, while increasing the gasper cross-sectional area can improve thermal comfort, a decrease in airflow velocity may lead to discomfort for the passenger in terms of thermal comfort.
- For modern helicopters, the air temperature and airflow into the cabin are determined by the pilots. However, there is no specific adjustment made for passenger thermal comfort in terms of temperature. As a result of this study, it has been concluded that if the air temperature is pre-determined based on the external environment temperature and integrated into the ECS system, optimal thermal comfort for passengers can be achieved.

As a continuation of this study, it is believed that the following areas could be beneficial for further research:

- The study can be expanded by increasing the number of passengers within the cabin and incorporating avionics equipment into the cabin.
- The analysis can be continued under different flight conditions and environments of the helicopter.

- The passengers' clothing has been considered as a fixed parameter. Since the clothing coefficient changes with different clothing, the variation in ET temperature can be investigated.
- The thermal load generated by passengers, along with factors such as gender, age, and seating position, can be investigated for their effects on thermal comfort.

REFERENCES

American Society of Heating, Refrigerating and Air-Conditioning Engineers. (2007). *ANSI/ASHRAE Standard 161-2007: Air quality within commercial aircraft*. ASHRAE.

American Society of Heating, Refrigerating and Air-Conditioning Engineers. (2013). *ANSI/ASHRAE Standard 161-2013: Air quality within commercial aircraft*. ASHRAE.

American Society of Heating, Refrigerating and Air-Conditioning Engineers. (2017). *ANSI/ASHRAE Standard 55-2017: Thermal environmental conditions for human occupancy*. ASHRAE.

Bosbach, J., Pennecot, J., Wagner, C., Raffel, M., Lerche, T., & Repp, S. (2006). Experimental and numerical simulations of turbulent ventilation in aircraft cabins. *Energy, 31*(5), 694–705.

Chun, C., Kwok, A., & Tamura, A. (2004). Thermal comfort in transitional spaces—Basic concepts: Literature review and trial measurement. *Building and Environment, 39*(10), 1187–1192.

Du, X., Li, B., Liu, H., Wu, Y., & Cheng, T. (2017). The appropriate airflow rate for a nozzle in commercial aircraft cabins based on thermal comfort experiments. *Building and Environment, 112*, 132–143.

European Union Aviation Safety Agency. (2024). *Certification specifications for large rotorcraft CS-29: Amendment 12*. EASA.

Fanger, P. O. (1970). *Thermal comfort: Analysis and applications in environmental engineering*. Danish Technical Press.

Frontczak, M., & Wargocki, P. (2011). Literature survey on how different factors influence human comfort in indoor environments. *Building and Environment, 46*(4), 922–937.

Houghten, F. C., Gutberlet, C., & Witkowski, E. (1938). *Draft temperatures and velocities in relation to skin temperature and feeling of warmth*. ASHVE Transactions.

International Organization for Standardization. (2005). *ISO 7730:2005: Ergonomics of the thermal environment—Analytical determination and interpretation of thermal comfort using calculation of the PMV and PPD indices and local thermal comfort criteria*. ISO.

ISO, E. (2006). Ergonomics of the thermal environment–Evaluation of thermal environments in vehicles–Part 2: Determination of equivalent temperature. ISO 14505-3: 2006.

Kühn, M., Bosbach, J., & Wagner, C. (2009). Experimental parametric study of forced and mixed convection in a passenger aircraft cabin mock-up. Building and Environment, 44(5), 961-970.

Li, J., Xiaodong, C., Junjie, L., Congcong, W., & Yongzhi, Z. (2015). Global airflow field distribution in a cabin mock-up measured via large-scale 2D-PIV. *Building and Environment, 93*(2), 234–244.

Liu, W., Wen, J., Chao, J., Yin, W., Shen, C., Lai, D., Lin, C.-H., Liu, J., Sun, H., & Chen, Q. (2012). Accurate and high-resolution boundary conditions and flow fields in the first-class cabin of an MD-82 commercial airliner. *Atmospheric Environment, 56*, 33–44.

Madsen, T. L. (1978). Measurement of thermal comfort and discomfort. Technical University of Denmark, Department of Civil Engineering.

Maier, J., Marggraf-Micheel, C., Dehne, T., & Bosbach, J. (2017). Thermal comfort of different displacement ventilation systems in an aircraft passenger cabin. *Building and Environment, 111*, 256-264.

Mboreha, C. A., Jianhong, S., Yan, W., Zhi, S., & Yantai, Z. (2021). Investigation of thermal comfort on innovative personalized ventilation systems for aircraft cabins: A numerical study with computational fluid dynamics. *Thermal Science and Engineering Progress, 26*, 101081.

Menter, F. R. (1994). Two-equation eddy-viscosity turbulence models for engineering applications. *AIAA Journal, 32*(8), 1598–1605.

Miracle, D. B., & Donaldson, S. L. (2001). *ASM handbook volume 21: Composites*. ASM International.

Moon, J. H., Lee, J. W., Jeong, C. H., & Lee, S. H. (2016). Thermal comfort analysis in a passenger compartment considering the solar radiation effect. *International Journal of Thermal Sciences, 107*, 77-88.

Rydberg, J., Norback, P., & Stockholm, S. (1949). Air distribution and draft. *ASHVE Transactions, 55*, 225.

SAE International. (2003). *SAE ARP292C: Environmental control systems for helicopters* (C ed.). SAE International.

SAE International. (2011). *SAE AIR 1168/3: Aerospace Information Report – Aerothermodynamic Systems Engineering and Design*. SAE International.

Wang, C., Liu, J., Li, J., Guo, Y., & Jiang, N. (2017). Turbulence characterization of instantaneous airflow in an aisle of an aircraft cabin mockup. *Building and Environment, 116*, 207–217.

Wang, L., Li, H., Zhang, Y., & Xu, C. (2024). A review of in-flight thermal comfort and air quality status in civil aircraft cabins. *Buildings, 14*(7), 2001.

Yan, W., Zhang, Y., Sun, Y., & Li, D. (2009). Experimental and CFD study of unsteady airborne pollutant transport within an aircraft cabin mock-up. *Building and Environment, 44*(1), 34–43.

You, R., Chen, J., Shi, Z., Liu, W., Lin, C.-H., Wei, D., & Chen, Q. (2016). Experimental and numerical study of airflow distribution in an aircraft cabin mockup with a gasper on. *Building Performance Simulation, 9*(5), 555–566.

Zhang, H., Dai, L., Xu, G., Li, Y., Chen, W., & Tao. (2008). Studies of air-flow and temperature fields inside a passenger compartment for improving thermal comfort and saving energy. Part I: Test/numerical model and validation. *Applied Thermal Engineering*, *28*(14-15), 1905–1917.

Zhang, T., & Chen, Q. Y. (2007). Novel air distribution systems for commercial aircraft cabins. *Building and Environment, 42*(4), 1675–1684.

Zítek, P., Vyhlídal, T., Simeunović, G., Nováková, L., & Čížek, J. (2010). Novel personalized and humidified air supply for airliner passengers. *Building and Environment, 45*(11), 2345-2353.

CURRICULUM VITAE

Name Surneme **:** Mehmet Külte

EDUCATION:

- **B.Sc.** **:** 2021, Istanbul Technical University, Mechanical Engineering

PROFESSIONAL EXPERIENCE AND REWARDS:

- 2021-2022 Arçelik A.Ş
- 2022-[Present] TUSAŞ (Turkish Aerospace Industries)

PUBLICATIONS, PRESENTATIONS AND PATENTS ON THE THESIS:

- **Külte M., Çadırcı S.** 2025. Numerical Investigaiton of Thermal Comfort for Passangers in a Helicopter Cabin. 15th International Conferance on Computational Heat & Mass Transfer, May 19-23, 2025 Antalya, Turkey.